UNIVERSITY OF
KWAZULU-NATAL

INYUVESI
YAKWAZULU-NATALI

Fumonisin B1 induces oxidative stress, mitochondrial dysfunction, mitophagy prevention and DNA hypermethylation in C57BL6 mice lung tissue

Anthia Camara Govender

220002745

Supervisor: Prof. A. A. Chuturgoon Co-supervisor: Dr. T. Ghazi

Submitted in fulfilment of the requirements for the degree of Master of Medical Science (Medical Biochemistry) in the Discipline of Medical Biochemistry, School of Laboratory Medicine and Medical Sciences, College of Health Science, University of KwaZulu-Natal, Durban

2024

Plagiarism Declaration

I, **Anthia Govender**, Student Number: ***220002745*** declare that:

i. The research reported in this dissertation, except where otherwise indicated, is my original work.

ii. This dissertation has not been submitted for any degree or examination at any other university.

iii. This dissertation does not contain other person's data, pictures, graphs or other information, unless specifically acknowledged as being sourced from other persons.

iv. This dissertation does not contain other person's writing, unless specifically acknowledged as being sourced from other researchers. Where other written sources have been quoted then:

   a. Their words have been re-written, but the general information attributed to them has been referenced.

   b. Where their exact words have been used, their writing has been placed inside quotation marks and referenced.

v. Where I have reproduced a publication of which I am an author, co-author or editor, I have indicated in detail which part of the publication was actually written by myself alone and have fully referenced such publications.

vi. This dissertation does not contain text, graphics or tables copied and pasted from the internet, unless specifically acknowledged, and the source is in the dissertation and in the reference sections.

Student Signed: [redacted] **Date:** 02 December 2024

Acknowledgements

My Family

I sincerely appreciate your unwavering love and support as well as your belief in my abilities and your encouragement in pursuing my dreams.

Professor A.A. Chuturgoon

I would like to express my gratitude for the opportunity to be involved in your research group as well as for your exceptional knowledge and guidance.

Dr T. Ghazi

I am truly grateful for your outstanding mentorship. The support and guidance you have provided have significantly enhanced my capabilities as a scientist.

Fellow Masters students (2024)

Thank you for your insightful suggestions and support. Best wishes for your future endeavours.

Discipline of Medical Biochemistry

I would like to express my gratitude to the Department of Medical Biochemistry, along with the staff and postgraduate students, for their invaluable support and assistance during the course of this project.

College of Health Sciences

Bursary and funding

Presentations

1. An evaluation of Fumonisin B1 induced mitochondrial dysfunction and mitophagy in C57BL/6 mice lung tissue. Govender A., Ghazi T., Chuturgoon A.A. School of Laboratory Medicine and Medical Sciences Research Day (27th September 2024), University of KwaZulu-Natal, Durban, South Africa.

Table of Contents

List of Figures

Chapter 2

Chapter 3

Chapter 4

Chapter 5

Appendix A

Appendix B

Appendix C

List of Tables

Chapter 3

Abbreviations

APS	Ammonium persulphate
ARE	Antioxidant response element
ATP	Adenosine triphosphate
BSA	Bovine serum albumin
CAT	Catalase
cDNA	Complementary deoxyribonucleic acid
Cers	Ceramide synthase
Cu^{+}	Cuprous ions
Cu^{2+}	Cupric ions
DNA	Deoxyribonucleic acid
dNTPs	Deoxynucleoside triphosphates
ETC	Electron transport chain
ELISA	Enzyme-linked immunosorbent assay
FB1	Fumonisin B1
Gpx	Glutathione peroxidase
GSH	Glutathione (reduced)
V	Volts
H_2O_2	Hydrogen peroxide
H_3PO_4	Phosphoric acid
HCl	Hydrogen chloride
HRP	Horse radish peroxidase
IARC	International Agency for Research on Cancer
Keap1	Kelch-like ECH-associated protein 1
LONP1	Lon-protease 1
MBD2	Methyl-CpG-binding domain
Mins	Minutes
MnSOD	Manganese-dependent superoxide dismutase
mRNA	Messenger ribonucleic acid
NQO1	NADPH-quinone oxidase
Nrf2	Nuclear-factor-erythroid 2 p45-related factor 2

O2•-	Superoxide radicals
OH	Hydroxyl
(ONOO)	Peroxynitrite
p62	Sequestosome 1
PBS	Phosphate-buffered saline
PCR	Polymerase chain reaction
Pink1	PTEN-induced kinase
qPCR	Quantitative polymerase chain reaction
ROS	Reactive oxygen species
RT	Room temperature
Sa	Sphinganine
SDS	Sodium dodecyl sulphate
SDS-PAGE	Sodium dodecyl sulphate–polyacrylamide gel electrophoresis
Sec	Seconds
SIRT 3	Sirtuin 3
SOD2	Superoxide dismutase 2
So	Sphingosine
TBARS	Thiobarbituric acid reactive substances
TEMED	Tetramethylethylenediamine
TTBS	Tween 20-Tris buffered saline
WHO	World Health Organisation

Abstract

Fumonisin B1 (FB1) is acknowledged as the most toxic variant of the *Fusarium* mycotoxins, largely due to its prevalence as a major naturally occurring fumonisin in agricultural products. The consumption of FB1 is associated with significant health risks for humans and animals. FB1 induces mitochondrial toxicity through the disruption of the mitochondrial electron transport chain (ETC), leading to mitochondrial membrane depolarization and an increase in reactive oxygen species (ROS) production. The aim of this investigation was to examine the mitochondrial toxicity in the lung tissue of mice treated with FB1 for 24 hours, along with the effects of FB1 on oxidative stress, mitophagy, and global DNA methylation. C57BL/6 mice (n=5/group) were orally administered 0.1 M phosphate-buffered saline (PBS) or 5mg/kg FB1 for 24 hours. Thereafter, the lungs were harvested, and RNA and protein were extracted. The TBARS assay was employed to measure lipid peroxidation. qPCR was used to corroborate the mRNA expression of oxidative stress-related genes [superoxide dismutase 1 (*SOD1*), superoxide dismutase 2 (*SOD2*), nuclear factor erythroid 2-related factor 2 (*Nrf2*), catalase (*CAT*) and glutathione peroxidase (*Gpx*)], mitochondrial stress mitigating and mitophagy related genes [sirtuin 3 (*Sirt3*), Lon peptidase 1 (*Lonp1*), PTEN-induced kinase 1 (*Pink1*), sequestosome 1 (*p62*), and *Parkin*] and DNA methylation-related genes [*DNMT1*, *DNMT3A*, *DNMT3B* and methyl-CpG-binding domain (*MBD2*)]. Western blot was used to establish the protein expression of SOD2, CAT, Sirt3, Lonp1 and Parkin. Global DNA Methylation was assessed by ELISA. Malondialdehyde (MDA) was significantly upregulated (p<0.0001) in the lung tissue of FB1-treated mice. Further, there was a marked decrease in the expression of antioxidant defence-related genes, including *Nrf2* (p<0.0001), *SOD1* (p=0.0003), and *Gpx* (p=0.0004). Additionally, there was a notable decrease in both the gene (p<0.0001) and protein (p<0.0001) expression of CAT, while SOD2 gene (p=0.7454) and protein (p=0.7141) expression did not show significant variation in the lungs of the treated mice, when compared to the controls. In terms of the mitochondrial stress response, FB1 significantly increased *Sirt3* transcripts (p=0.0244) and protein expression (p=0.0001), coupled with a significant decrease in Lonp1 gene (p<0.0001) and protein (p<0.0001) levels. Moreover, following FB1 treatment, significant reductions were observed in the expression of *Pink1* (p<0.0001), *Parkin* (p=0.0162), and *p62* (p<0.0001) genes, alongside a significant decrease in Parkin protein (p<0.0001) expression. Finally, a significant increase in both global DNA methylation (p=0.0018) and expression of *DNMT3A* (p=0.0082) and *DNMT3B* (p=0.0047) was noted; *DNMT1* (p=0.1521) and *MBD2* (p=0.6934) expressions showed no significant change in the lung tissue of FB1-treated mice, relative to controls. FB1 disrupted mitochondrial function and inhibited mitophagy in mouse lungs. Furthermore, it induced oxidative stress, that contributed to mitochondrial toxicity and global DNA hypermethylation.

Keywords: Fumonisin B1, Mitochondrial dysfunction, Oxidative stress, Mitophagy, DNA methylation.

Chapter 1: Introduction

1.1 Background

Recently, the issue of global food security has been notably undermined by the rising danger of mycotoxin contamination. Mycotoxins, which are secondary metabolites produced by fungi, are naturally occurring and frequently found in a range of agricultural food products, posing a serious risk to the health of both humans and animals (Omotayo *et al*., 2019). Various types of mycotoxins, such as aflatoxins, ochratoxins, patulin, and fumonisins, can be detected in agricultural products. Among these mycotoxin variants, fumonisin has been identified as a causative agent of fatal diseases in both humans and animals (Sheik Abdul and Marnewick, 2020). Fumonisins are classified as polyketide mycotoxins that are mainly generated by the fungus *Fusarium verticillioides*, a common contaminant of crops such as corn and wheat (Bush *et al*., 2004). Previous studies have recognized more than 15 variations of fumonisins, with FB1 being considered the most hazardous, as it is frequently found in a wide range of agricultural products (Domijan, 2012). The ingestion of corn and wheat produce that have been contaminated with FB1 can result in a range of health issues for both animals and humans. Studies have demonstrated that exposure to FB1 in humans is associated with the occurrence of neural tube defects, along with a heightened risk of oesophageal and liver cancers (Goksun *et al*., 2015, Alizadeh *et al*., 2012).

Recently, studies have shown mitochondrial dysfunction as a potential mechanism of FB1 toxicity (Sheik Abdul and Marnewick, 2020). Oxidative stress is a mechanism through which FB1 promotes mitochondrial dysfunction. FB1 was discovered to have a toxic effect by stimulating increased generation of ROS in the mitochondria, while simultaneously impairing cellular antioxidant defences, which ultimately results in mitochondrial dysfunction (Arumugam *et al*., 2018). The lung is an organ that demands significant levels of energy and is abundant in mitochondria (Sureshbabu and Bhandari, 2013). The onset of lung injury and the development of lung diseases have been associated with mitochondrial dysfunction caused by elevated ROS production (Vikas, 2018). Understanding the molecular and cellular mechanisms resulting in FB1-induced mitochondrial dysfunction is essential to develop therapeutic approaches.

Numerous health issues have been associated with mitochondrial dysfunction, especially in tissues that require a lot of energy (Yildirim *et al*., 2022). Because of the vital role the mitochondria play in producing cellular energy, mechanisms such as mitophagy and the promotion of mitochondrial biogenesis are used to carefully regulate biological balance. When exposed to toxins, the mitochondria engage in the activation of antioxidant and stress mitigating responses (Mohan *et al*., 2022). The mitochondrial proteins Lonp1 and Sirt3 are stimulated to uphold proper mitochondrial function (Gibellini *et al*., 2014, Zanini *et al*., 2023). When mitochondrial stress cannot be relieved, it triggers the process of mitophagy. Mitophagy is a crucial subtype of autophagy that degrades dysfunctional mitochondria, ensuring the cell's overall functionality is maintained (Wen *et al*., 2022). The proteins Pink1 and p62 are crucial in mitophagy and are influenced by various factors. Understanding the molecular and cellular effects that FB1 has on mitophagy is essential to develop therapeutic approaches.

DNA methylation is a well-studied epigenetic process where DNA methyltransferases (DNMTs) add methyl groups to the C-5 position of the cytosine ring in DNA (García-Guede *et al*., 2020). DNA methylation plays a crucial role in proper developmental processes. Disruption in its regulation has been linked to various diseases, including cancer (Menezo *et al*., 2016). Prior research has demonstrated that folate deficiency induced by FB1 can lead to alterations in DNA methylation patterns, which may contribute to cancer development (Goksun *et al*., 2015). Studies have revealed that higher levels of ROS production can result in changes in DNA methylation levels (Gao *et al*., 2019). Although it is biologically plausible, there is not enough evidence showing a clear link between FB1-induced oxidative stress and its effects on DNA methylation regulation.

Previous research has examined the impact of FB1 on mitochondrial dysfunction, oxidative stress and DNA methylation; however, the specific effects of FB1 on these pathways and its potential role in contributing to lung injury remain underexplored. Furthermore, the existing literature reveals a significant gap in research concerning the effects of FB1 on mitophagy. A comprehensive understanding of the molecular and cellular ramifications of FB1 on oxidative stress, mitochondrial dysfunction, mitophagy, and DNA methylation in lung tissue is vital for the advancement of therapeutic interventions.

1.2 Problem Statement / Rationale

Mycotoxin contamination has become a major concern for food security worldwide. Mycotoxins contaminate food and agricultural products causing various health issues in animals and humans. They cannot be eradicated from contaminated agricultural products because they are resistant to heat, posing a high risk of ingestion by humans and animals. Mycotoxins pose a danger to human health because they can lead to serious and irreversible conditions such as cancer. FB1 has been recognized as the most toxic fumonisin analogue, as it is a major naturally occurring fumonisin in agricultural foods. FB1 has been found to weaken the quality of agricultural products leading to reduced food intake and yield, ultimately resulting in a decline in the economy. Animals that have ingested FB1-contaminated feed have been found to experience health problems such as pulmonary oedema and Leukoencephalomalacia (Vendruscolo *et a*l., 2016). Evidence also suggests that FB1 possesses carcinogenic properties that are responsible for the development of oesophageal cancer predominantly in areas that consume high corn and maize-based diets. Pregnant women who consume high levels of FB1-contaminated food during the early stages of pregnancy face an increased likelihood of delivering infants with neurological and spinal cord anomalies (Chen *et al*., 2021). Understanding the molecular and cellular mechanisms resulting in FB1-induced health problems is essential to develop therapeutic approaches.

1.3 Significance/ Implications

There is very little that can be done to prevent and reverse FB1 contamination of agricultural foods. This is a result of FB1's water soluble nature and its ability to resist heat of normal cooking temperatures (Chen *et al*., 2021). This increases the risk of humans and animals ingesting contaminated products and FB1 inducing a toxic effect that may result in severe health problems. Research is thus warranted to understand FB1 mechanisms of toxicity and develop treatment/prevention methods. The primary mechanism through which FB1 exerts its toxic effects has been recognized as its capacity to interfere with sphingolipid metabolism. Over time, a substantial amount of evidence has emerged, suggesting that mitochondria could be a primary target of FB1 toxicity. Despite existing studies, the influence of FB1 on the mitochondria is not thoroughly comprehended. Since the lung is abundant in mitochondria, studying how FB1 can cause mitochondrial dysfunction through oxidative stress and its effect on mitophagy is crucial. In terms of FB1-mediated epigenetic effects, prior research has indicated that folate deficiency induced by FB1 can lead to alterations in DNA methylation and contribute to FB1-induced carcinogenesis (Goksun *et al*., 2015). FB1-induced mitochondrial dysfunction and excess ROS production may influence DNA methylation levels. Research has shown that an upregulation in the generation of ROS can lead to changes in DNA methylation levels (Gao *et al*., 2019). Despite the biological plausibility, there is limited evidence regarding the connection between FB1-induced oxidative stress and its impact on DNA methylation regulation. Additionally, there is a paucity of information on the ability of FB1-induced oxidative stress to disrupt DNA methylation and potentially contribute to carcinogenesis.

1.4 Research questions

- Does FB1 cause oxidative stress in C57BL/6 mice lung tissue?
- Does FB1 induce mitochondrial dysfunction/mitophagy in C57BL/6 mice lung tissue?
- Does FB1 alter global DNA methylation levels in C57BL/6 mice lung tissue?

1.5 Hypothesis

FB1 increases oxidative stress and impairs mitochondrial function, which in turn activates mitophagy and causes DNA hypermethylation in mice lungs.

1.6 Aim

This study aimed to examine the effect of FB1 on oxidative stress, mitochondrial dysfunction, mitophagy and global DNA methylation in C57BL/6 mice lung tissue following 24 hours exposure.

1.7 Objectives

The objectives of this study are:

- To determine the effect of FB1 on oxidative stress in mice lung tissue by:
  - quantifying lipid peroxidation using the Thiobarbituric acid reactive substances (TBARS) assay.
  - detecting the expression of antioxidant genes *SOD1, SOD2, Gpx, CAT* and oxidative stress markers such as *Nrf2* by qPCR.
  - detecting the protein expression of antioxidant enzymes SOD2 and CAT by western blot.
- To determine the effect of FB1 on mitochondrial dysfunction/mitophagy by:
  - detecting the expression of specific genes involved in mitigating mitochondrial stress and mitophagy such as *Sirt3, Lonp1, Pink 1, Parkin* and *p62* using qPCR.
  - detecting protein expression of Sirt3, Lonp1 and Parkin using western blot.
- To determine the effect of FB1 on DNA methylation by:
  - quantifying global DNA methylation levels using an ELISA
  - detecting gene expression of *DNMTs* and *MBD2* using qPCR.

Chapter 2: Literature Review

2.1 Mycotoxins

The contamination of agricultural products is often attributed to mycotoxins, which are naturally occurring secondary metabolites produced by fungi. There are many variants of mycotoxins such as ochratoxins, aflatoxins, patulin and fumonisins (Figure 2.1). Various species of fungi contribute to the production of mycotoxin variants. For example, aflatoxin and ochratoxin can be produced by numerous fungal species, resulting in the presence of mycotoxins throughout the year (Hussein, 2001). Mycotoxins have structural variations and different toxicity levels, which depend on the amount and duration of exposure. The World Health Organization (WHO) has classified certain mycotoxins as human carcinogens or teratogens (World Health, 2023). However, nearly all mycotoxins can lead to significant health issues due to contamination of staple foods such as corn, wheat, and rice. Contamination can occur during the cultivation and harvesting processes in agricultural fields as well as during the storage phase. Once agricultural products are contaminated with mycotoxins, these toxins cannot be removed, as they are water-soluble and resistant to heat generated by normal cooking temperatures (Chen *et al*., 2021). This poses a risk to both humans and animals, as consuming contaminated products can lead to toxic effects that may result in severe health problems.

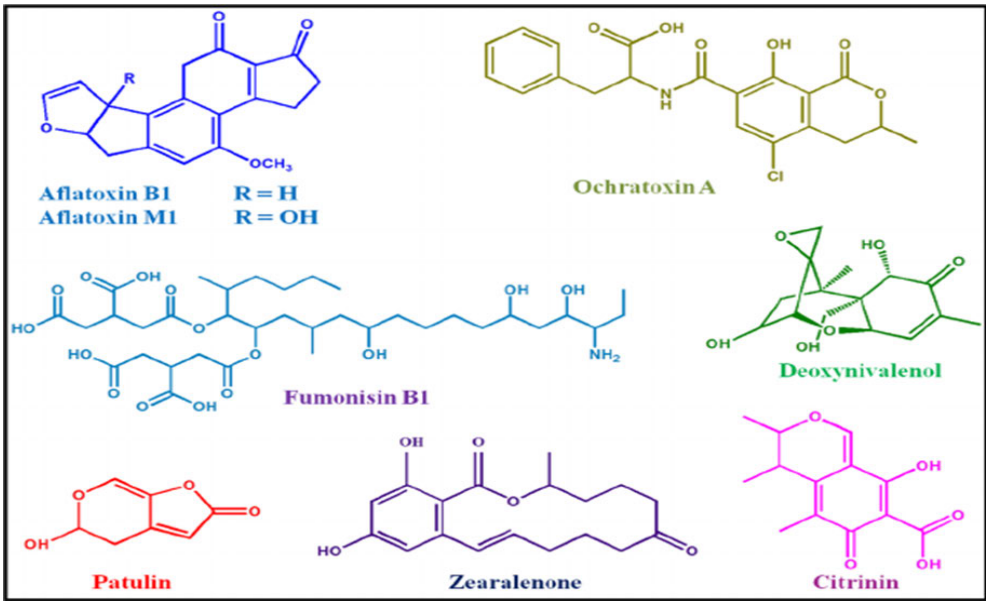

Figure 2.1: Chemical structures of commonly produced mycotoxins (Malhotra *et al*., 2014).

The synthesis of fumonisins is mainly attributed to certain species within the *Fusarium* genus, particularly *Fusarium verticillioides* and *Fusarium proliferatum* (Yazar and Omurtag, 2008). While fumonisins are mainly linked to contamination in maize, they have also been identified as contaminants in other agricultural products, such as rice and sorghum (Shephard *et al*., 1996). Research undertaken in South Africa that involved the extraction of fumonisins from the *Fusarium moniliforme* strain MRC 826 found the mycotoxin to induce Leukoencephalomalacia in horses and hepatocellular carcinoma in rats (Gelderblom *et al*., 2008). Previous investigations have shown that there are over 28 different fumonisins, which can be classified into four distinct groups based on their chemical composition: FA, FB, FC, and FP (Rheeder *et al*., 2002).

2.1.1 Fumonisin B1

Among the fumonisin analogues identified, FB1 has been found to be the most toxic, as it is a major naturally occurring fumonisin in agricultural products (Sheik Abdul and Marnewick, 2020). The ingestion of maize and grain products contaminated with FB1 causes many illnesses in both animals and humans (Figure 2.2). In 2002, the maximum tolerable daily dose of FB1 was identified to be 2 µg/kg body weight (World Health, 2023). FB1 has been designated as a group 2B carcinogen by the International Agency for Research on Cancer (IARC) (Iarc, 2002). There is evidence that FB1 may contribute to oesophageal cancer predominantly in areas that consume high maize-based diets (Alizadeh *et al*., 2012, World Health, 2023). The molecular structure of FB1 consists of diesters of tricarballylic acid with a polyhydric alcohol backbone (Figure 2.1) (Gelderblom *et al*., 2008).

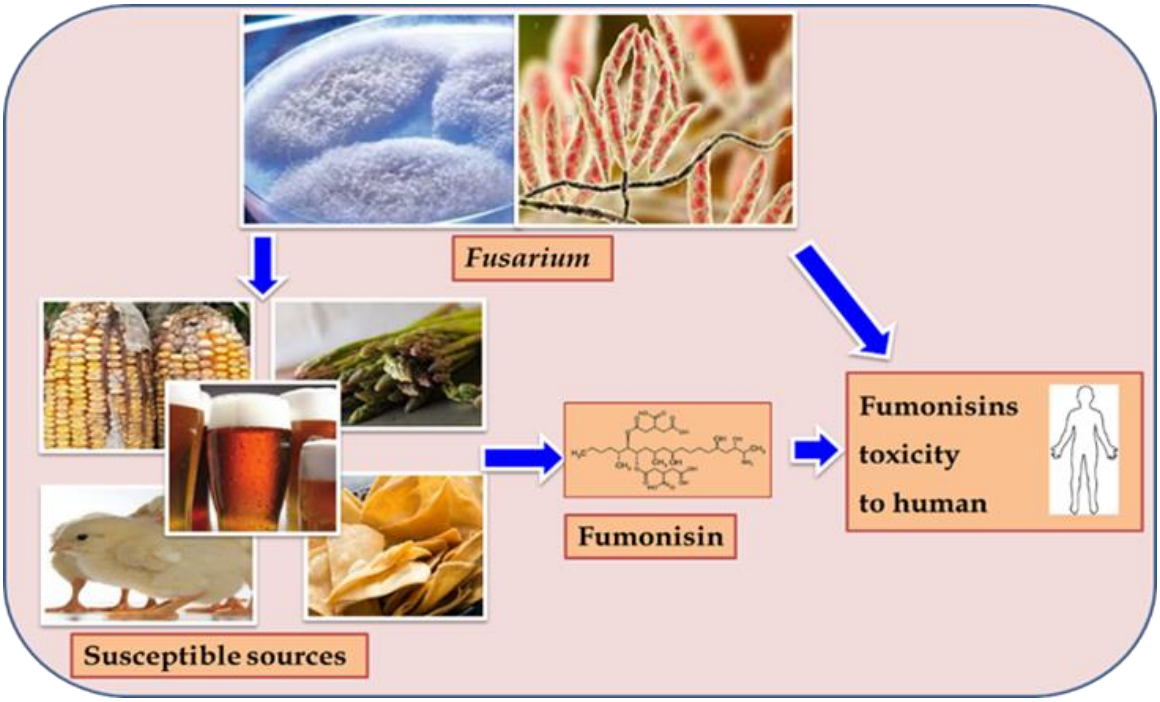

Figure 2.2: Fumonisin and its impact on agriculture, food and humans (Kamle *et a*l., 2019).

2.1.2 Mechanism of action

FB1 has a structure similar to sphingosine (So), which allows it to disrupt sphingolipid metabolism by competing with So for ceramide synthase (Cers). This competition leads to decreased levels of ceramide, dihydroceramides, and complex sphingolipids, contributing to the mechanism of FB1 toxicity (Figure 2.3) (Chen *et al*., 2021). At the cellular level, FB1 initiates an increase in sphinganine (Sa) levels and a rise in the Sa to So ratio; these serve as biomarkers for identifying exposure to FB1 (may be identified through analysis of tissues, serum, and urine) (Merrill *et al*., 2001). Another study suggested sphingosine-1-phosphate (So-1-phosphate) as a useful biomarker, as it showed higher levels than So and Sa in their findings (Chen *et al*., 2021). Diseases in which fumonisins disrupt sphingolipid biosynthesis are classified as "sphingolipidosis", due to their correlation with alterations in lipidomic profiles and associated biological functions (Riley and Merrill, 2019). A significant quantity of sphingolipids can be found within the cell membrane, where they are essential for maintaining the structural integrity of the membrane (Merrill *et al*., 2001). Complex sphingolipids, found in the cellular membranes, serve as important precursors for second messenger molecules and play a critical role in supporting cellular growth and differentiation. FB1-induced disruption in sphingolipid metabolism has been found to cause changes in cell signalling resulting in cytotoxic effects, apoptosis, and oxidative stress.

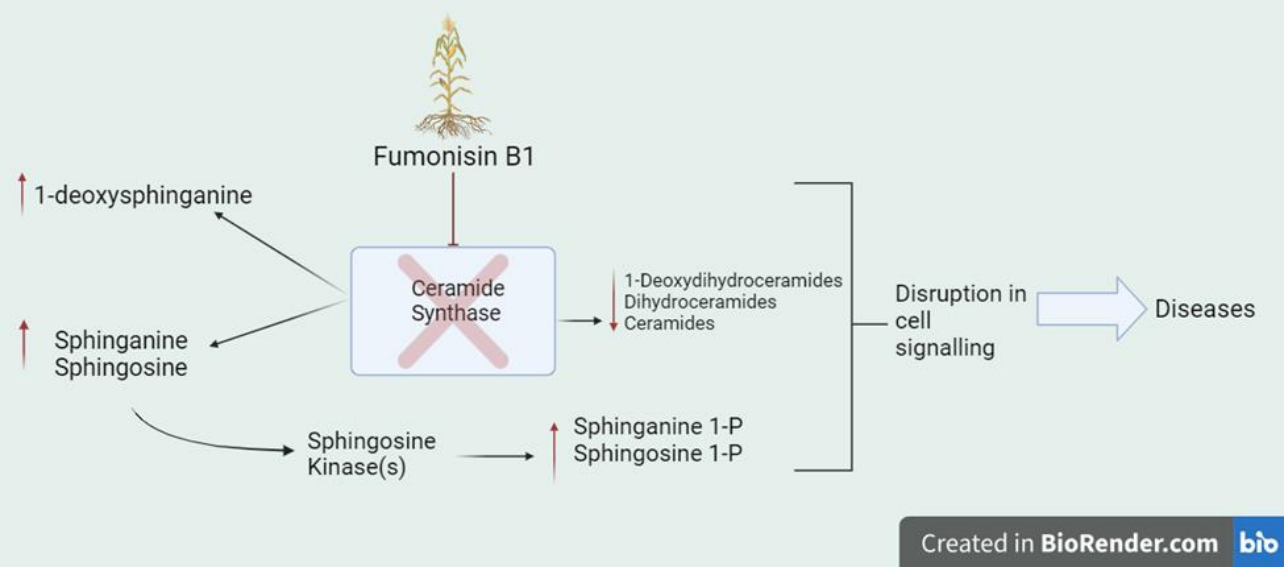

Figure 2.3: Changes induced by FB1 because of ceramide synthase inhibition (prepared by author).

2.1.2.1 Animals

Numerous research studies have investigated the biochemical mechanisms underlying diseases induced by FB1 in animals (Figure 2.4). FB1 has been found to induce toxic effects by targeting the brains of horses and the lungs of pigs. It was found to cause severe liver damage in both species, pancreatic lesions, and pulmonary oedema in pigs as well as Leukoencephalomalacia in horses (Vendruscolo *et al*., 2016, Haschek *et al*., 2001). FB1 also caused brain haemorrhage in rabbits and hepatotoxic and carcinogenic effects in rats (Domijan, 2012, Gelderblom *et al*., 2008) .

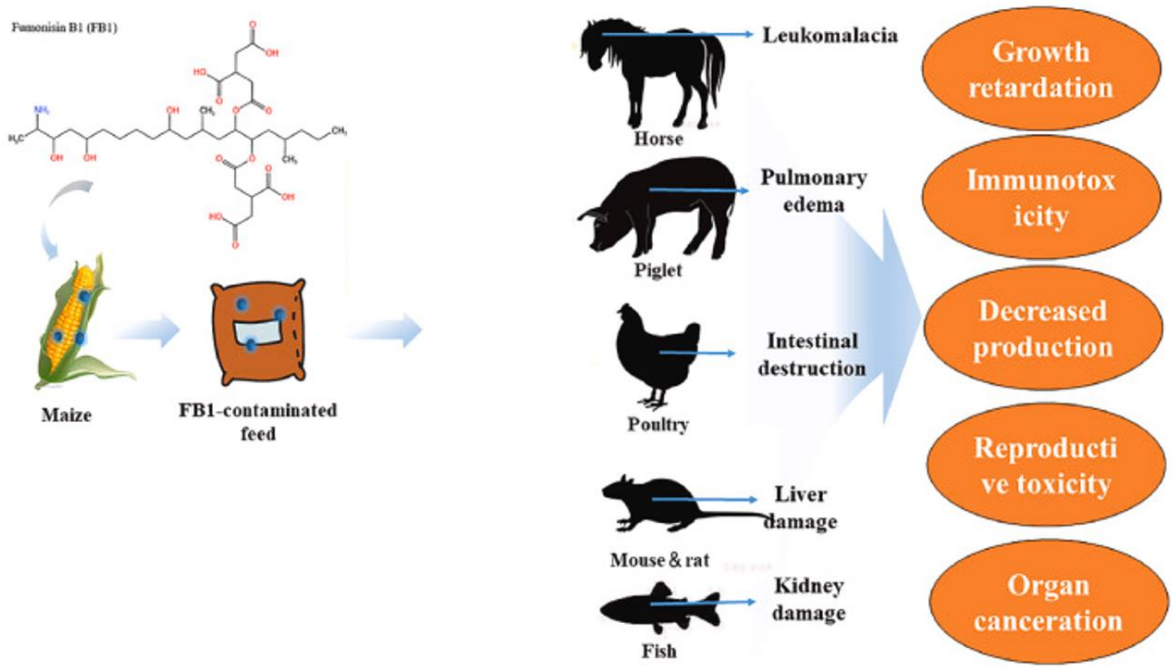

Figure 2.4: FB1 impact on animals and its toxic effects (Gao *et al*., 2023).

2.1.2.2 Humans

In humans, FB1 was found to induce neural tube defects (Domijan, 2012). Pregnant women that consumed high levels of FB1 contaminated food during the early stages of pregnancy were at an increased risk of delivering infants with congenital anomalies affecting the brain and spinal cord (Kamle *et al*., 2019, Waes *et al*., 2009). Evidence also suggests that FB1 possesses carcinogenic properties that can lead to oesophageal cancer, predominantly in areas that consume a high maize-based diet (Alizadeh *et al*., 2012, World Health, 2023). FB1 also increases the risk of heart failure in humans, as it causes damages in myocardial contractility as well as massive blood influx (Stoev, 2015). While it is known that FB1 can result in pulmonary edema in porcine subjects, there exists a considerable gap in the literature concerning its effects on human lung function. Major gaps in the research on FB1 in humans can be attributed to the insufficient availability of comprehensive data on human exposure levels, a limited understanding of how it is absorbed and metabolised in the human body, and the absence of established biomarkers for exposure (Alvito *et al*., 2022).

2.1.3 Molecular toxicity

2.1.3.1 Mitochondrial dysfunction and oxidative stress

The mitochondrion is an essential organelle, often referred to as the cell's powerhouse, due to its crucial function in generating energy in the form of ATP (Pieczenik and Neustadt, 2007). The mitochondria are a target of FB1 toxicity; one way FB1 induces mitochondrial dysfunction is by altering mitochondrial calcium homeostasis (Sheik Abdul and Marnewick, 2020). Mitochondrial dysfunction can also occur by FB1 interfering with the ETC (Rumora *et al*., 2007). The ETC consists of five protein complexes (I, II, III, IV, V) located within the mitochondria, three (I, III, IV) of which provide the necessary proton motive force for ATP synthase (Ahmad *et al*., 2018). FB1 is an inhibitor of mitochondrial complex 1 and has also been found to significantly downregulate state 3 and state 4 mitochondrial respiration (Domijan *et al*., 2012). It also induces toxicity by increasing ROS production in the mitochondria and impairing cellular antioxidant responses resulting in mitochondrial dysfunction (Arumugam *et al*., 2018, Domijan, 2012, Khan *et al*., 2018).

2.2 Oxidative Stress

Oxidative stress is referred to as an imbalance between the generation of free radicals and antioxidant defences (Burton and Jauniaux, 2011).

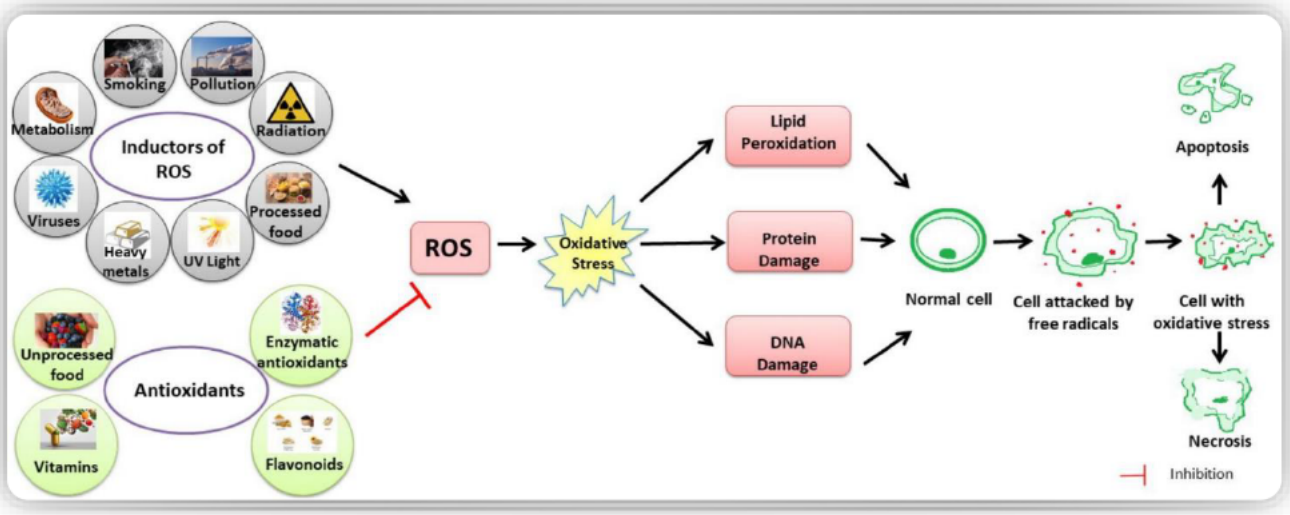

Figure 2.5: ROS sources and their connection to oxidative stress (Sharifi-Rad *et al*., 2020).

2.2.1 Free radicals and oxidants

Free radicals are oxygen and nitrogen molecules with one or more unpaired electrons in their outer orbital; they are highly reactive and unstable molecules. A balance among free radicals and antioxidants is important in terms of maintaining appropriate physiological function. In small amounts (physiological levels), free radicals serve important functions such as helping the body to combat inflammation, eliminate bacteria and control smooth muscles that ensure the correct functioning of internal organs and blood vessels (Qazi, 2018). However, when the generation of free radicals surpasses the cells antioxidant capacity, it leads to oxidative stress. ROS and reactive nitrogen species (RNS) serve as prominent examples of free radicals. ROS originate from both endogenous and exogenous sources. The mitochondria, endoplasmic reticulum and phagocytic cells are considered endogenous sources. An example of ROS generated by endogenous sources include superoxide anion. Exogenous sources that produce free radicals are pollution, alcohol, tobacco smoke, heavy metals, and pesticides (Figure 2.5) (Phaniendra *et al*., 2014). Examples of ROS that are produced by exogenous sources are superoxide anion ($^{\bullet}O_2$), hydrogen peroxide (H_2O_2), and hydroxyl radical ($HO^{\bullet}$). RNS are produced when the enzyme nitric oxide (NO) converts L-arginine into L-citrulline, this process produces NO. The formation of RNS can also occur when N-nitrosamines form from nitrates and nitrites. This occurs in the gut when nitrates and nitrites from the food eaten are converted into nitrosamines, which are reactive species. NO can react with superoxide to form peroxynitrite (ONOO) which is a potent RNS.

2.2.2 Antioxidants

Stabilization of free radicals can be achieved by using antioxidants. Antioxidants are molecules that can donate electrons to free radicals without compromising their own stability (Liu, 2023). In order to deal with oxidative stress, both enzymatic and non-enzymatic antioxidant systems are necessary for a cellular response to occur. CAT, SOD and GSH-PX (Figure 2.6) are examples of enzymatic antioxidants. Examples of non-enzymatic antioxidants are glutathione (GSH), and vitamins C and E (Figure 2.5).

Manganese-dependent superoxide (MnSOD) commonly referred to as SOD2 is an enzyme present in humans and encoded by the *SOD2* gene, situated on chromosome 6 (Gupta *et al*., 2023). The SOD2 enzyme can lower ROS and provide protection against cell death by removing toxic superoxide radicals produced during the mitochondrial ETC and converting them into H_2O_2 and diatomic oxygen (Ngo and Duennwald, 2022). Antioxidant enzymes such as CAT and Gpx are also important (Pei *et al*., 2023, Li *et al*., 2015). These antioxidant enzymes are responsible for the detoxification of H_2O_2.

The enzyme CAT is found in the peroxisomes of all living organisms that encounter oxygen and functions to degrade H_2O_2 into water and oxygen (Pei *et al*., 2023). The enzyme Gpx is an essential class of selenoenzymes in mammals. The Gpx antioxidant enzyme uses low molecular weight thiols such as GSH as cofactors to detoxify H_2O_2 into water and oxygen.

Nuclear factor erythroid 2-related factor 2 (Nrf2) has been found to regulate the transcription of the above mentioned antioxidant enzymes, in an effort to reduce oxidative stress (Ngo and Duennwald, 2022). The Kelch-like ECH-associated protein 1 (Keap1) -Nrf2 pathway serves as the predominant antioxidant defence mechanism in response to oxidative stress. Under normal conditions, the activity of Nrf2 is controlled through its association with Keap-1 (Baird and Yamamoto, 2020). When bound to Keap1, Nrf2 stays in the cytoplasm, where it is marked for ubiquitination and subsequent proteasomal degradation. However, under stressful conditions Keap1 cytosine residues are disrupted, which causes Nrf2 to detach from the Keap1 protein and is translocated to the nucleus rather than being degraded. Once inside the nucleus, Nrf2 can help reduce stress by facilitating the transcription of several genes that reduce stress, such as antioxidant enzymes (Gumeni *et al*., 2021, Youle and Narendra, 2010)

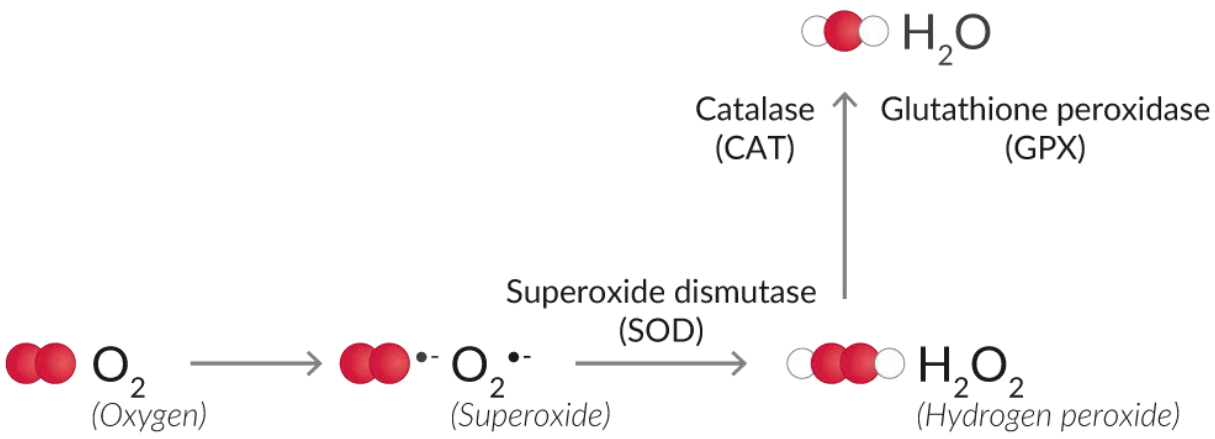

Figure 2.6*:* Detoxification of $O_2^{\bullet-}$ by SOD, Gpx and CAT (Cayman, 2022) .

2.3 Mitochondrial dysfunction

Mitochondria are membrane-bound organelles that produce majority of chemical energy required to drive biochemical reactions within cells (Pieczenik and Neustadt, 2007). Mitochondrial dysfunction results from either an insufficient quantity of mitochondria, a failure to supply them with essential substrates, or impairment in their electron transport and ATP synthesis mechanism. Reduced energy production is the most notable effect of mitochondrial dysfunction. However, during dysfunction,

there is also an increase in the generation of free radicals and exothermic oxygen combustion which results in cellular damage.

2.3.1 Mitochondrial stress mechanism

Mitochondrial dysfunction is related to a wide range of pathologies, especially in tissues with high energy demands (Yildirim *et al*., 2022). Due to the vital role mitochondria play in cellular energy production, the maintenance of homeostasis is meticulously controlled through processes such as mitochondrial biogenesis and mitophagy. When exposed to toxins, the mitochondria engage in the activation of antioxidants and stress mitigating responses (Mohan *et al*., 2022). Lonp1 and Sirt3 are examples of mitochondrial proteins that are stimulated to uphold proper mitochondrial function (Gibellini *et al*., 2014, Zanini *et al*., 2023).

Sirt3 is an important deacetylate present in the mitochondrial matrix and is responsible for the activation and inhibition of several proteins (Zhang *et al*., 2020). This ability has made Sirt3 an important modulator of multiple pathways (Bause and Haigis, 2013). It has been found to target enzymes in the citric acid cycle such as isocitrate dehydrogenase 2 and aconitase as well as enzymes in oxidative phosphorylation (OXPHOS) such as complex 1 and 2 of the ETC. In addition to metabolic regulation, Sirt3 is crucial for controlling ROS generation in the mitochondria (Bause and Haigis, 2013). This is done via the deacetylation and acetylation of MnSOD, which is responsible for scavenging ROS to reduce oxidative stress. Research has demonstrated that mitochondrial stress conditions can result in increased Sirt3 protein and gene expression, and the inhibition of Sirt3 can hinder the improvement of mitochondrial stress and cause cell death (Weir *et al*., 2013). Upregulation of Sirt3 expression is influenced by the degree of stress present, and an increase in stress coincides with an upregulation of Sirt3 expression.

The Lonp1 protease is a member of the human mitochondrial AAA^+ family and is essential for controlling diverse aspects of mitochondrial biology such as ETC activity and mitochondrial transcription (Shin *et al*., 2021). The ATP-dependent protease Lonp1 also has a significant role in the mitochondrial proteolytic system as it actively oxidises matrix proteins to prevent their accumulation within the mitochondria (Zanini *et al*., 2023). Sirt3 post-transcriptionally regulates Lonp1. Protein expression is reduced when Sirt3 deacetylates Lonp1. Sirt3 silencing results in an increase in Lonp1 protein expression; however, Sirt3 does not affect the activation or suppression of Lonp1 gene expression (Gibellini *et al*., 2014).

2.3.2 Mitophagy

The inability to alleviate mitochondrial stress or toxicity leads to the process of mitophagy. Mitophagy is a type of autophagy that functions to break down impaired mitochondria to preserve the overall functionality of the cells (Wen *et al*., 2022). Mitophagy was first identified in mammalian cells, where there was a notable increase in the sequestration of mitochondria by lysosomes after the administration of glucagon (Youle and Narendra, 2010). The p62 and Pink1 proteins are crucial for mitophagy and are controlled by a variety of factors (Mohan *et al*., 2022). Under normal conditions, the protein Parkin is in the cytosol. However, during stress Parkin moves into the mitochondria due to depolarization of the mitochondrial membrane (Wen *et al*., 2022). Healthy cells contain minimal amounts of Pink1 due to its proteolytic processing and degradation by PARL within the inner mitochondrial membrane. Mitochondrial damage results in the depolarization of the inner membrane, this prevents Pink1 from entering the mitochondrial matrix, where it is broken down. As a result, the Pink1 protein accumulates on the outer membrane, where it causes Parkin to become active (Yildirim *et al*., 2022). Subsequently, the protein Parkin can initiate mitophagy by ubiquitinating multiple proteins on the outer membrane of the mitochondria.

The p62 protein is a vital regulator present in the cytoplasm that behaves as a selective autophagy receptor for the breakdown of ubiquitinated substrates (Gureev *et al*., 2020). By polymerizing with additional p62 molecules, it can aggregate ubiquitylated structures and recruit them to phagosomes by binding to the LC3 protein. Similarly, p62 binds to Parkin mitochondrial substrates and permits ubiquitylated mitochondria to cluster together (Geisler *et al*., 2010, Narendra *et al*., 2010). The p62 protein influences Nrf2 function by binding to its negative regulator Keap1 and inducing the activation of Nrf2. It has been demonstrated to be a promoter of mitophagy as Nrf2 transcriptionally activates the upregulation of Pink1 and p62. Nrf2 transcriptionally controls the expression of the Pink1 gene by activating the antioxidant response element (ARE) located within the promoter region of Pink1. Evidence suggests that the Nrf2-Pink1-p62 pathway plays a crucial role in facilitating cell survival (Gumeni *et al*., 2021).

2.4 DNA Methylation

Epigenetics is the study of how external factors can modify gene expression without altering the actual DNA sequence (Baccarelli and Bollati, 2009). Epigenetic modifications refer to alterations in the structure of DNA that influence the activation or suppression of genes. DNA methylation is an important epigenetic mechanism that has been thoroughly investigated and is broadly accepted. It is an epigenetic modification that involves the enzymatic transfer of methyl groups from S-adenosyl methionine (SAM) to the C-5 position of the cytosine ring in DNA, a reaction catalysed by DNA methyl transferases (DNMTs) (García-Guede *et al*., 2020, Jin *et al*., 2011, Menezo *et al*., 2016). Within the DNMT enzyme classification there are three primary types, DNMT3A and DNMT3B are primarily engaged in the *de novo* methylation process of DNA. Whereas DNMT1 is responsible for the preservation of methylation patterns post DNA replication (Jin *et al*., 2011, Menezo *et al*., 2016). An example of an identified epigenetic regulator that influences gene expression is the MBD2 protein. MBD2 transcriptionally repress genes by interacting with CpG islands in promoter regions, by relying on the presence of methylation (Berger and Bird, 2005). DNA methylation is essential for normal cell functions. Research has shown that an increase in the production of ROS can lead to alterations in DNA methylation levels (Gao *et al*., 2019). For instance, hydrogen peroxide deprotonates the cytosine molecule at the C-5 position by acting as a nucleophile. This speeds up the reaction between DNA and SAM, which is important in the DNA methylation process. ROS can also control the expression of DNMTs, and dysregulation of these enzymes can lead to DNA hypomethylation. Based on the above findings, it can be inferred that oxidative stress may play a role in the disruption of DNA methylation regulation.

2.5 The Lungs

The lungs are a pair of spongy-pinkish-grey organs located in the chest (thorax), below the rib cage and above the diaphragm (National Heart and Blood, 2022). The right lung has 3 lobes, and the left lung is divided into 2 lobes (Figure 2.7). These lobes are further subdivided into over 30 million alveoli, which are very small air sacs where the exchange of oxygen and carbon dioxide takes place. Every cell in the body requires oxygen to function and live (Walker, 2022). The oxygen that is obtained from the environment enters the lungs during a process known as breathing, and gets transported through the alveoli into the bloodstream, which transports oxygen throughout the body (National Heart and Blood, 2022).The respiratory system is supported by the circulatory system which helps deliver nutrients and oxygen from the lungs to tissue and organs throughout the body. The oxygen is then exchanged at the cellular level and carbon dioxide is removed from the cells as waste. The carbon dioxide that is removed is then transported back to the lungs via the bloodstream where it is exhaled. The lungs and respiratory system automatically perform this vital process known as gaseous exchange (National Heart and Blood, 2022).

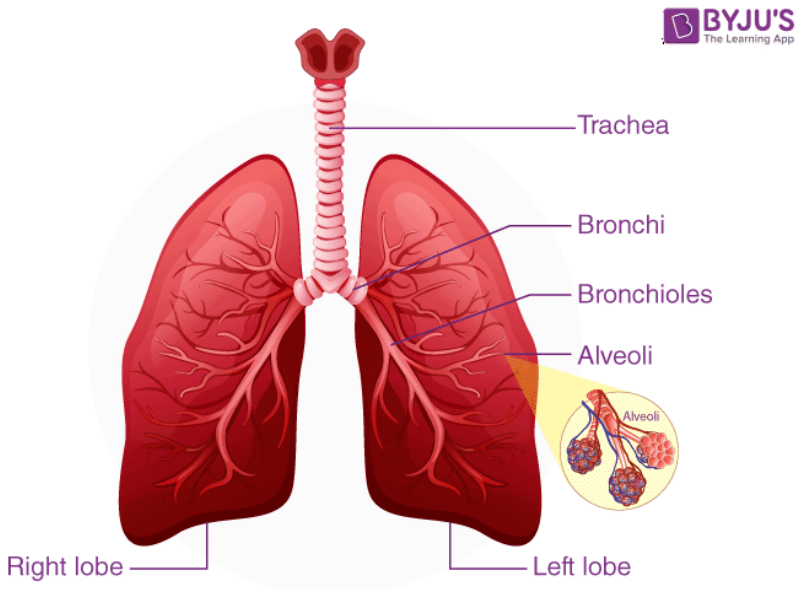

Figure 2.7: Structure of the lungs (BYJU's, 2023).

2.5.1 The lung and mitochondrial dysfunction

Mitochondria are important organelles that facilitate cell metabolism, promote growth, and ensure functional integrity (Pieczenik and Neustadt, 2007). The mitochondria found in lung cells are vital for the regulation of proper lung function, as they are involved in key processes such as the synthesis of surfactant and regeneration (Zhan and Shen, 2022). Impairment of these mitochondrial processes has the potential to lead to various pathophysiological conditions such as asthma (Figure 2.8). Research indicates that mitochondrial dysfunction within the lung is attributed to elevated ROS production, exposure to cigarette smoke as well as mitochondrial depolarization.

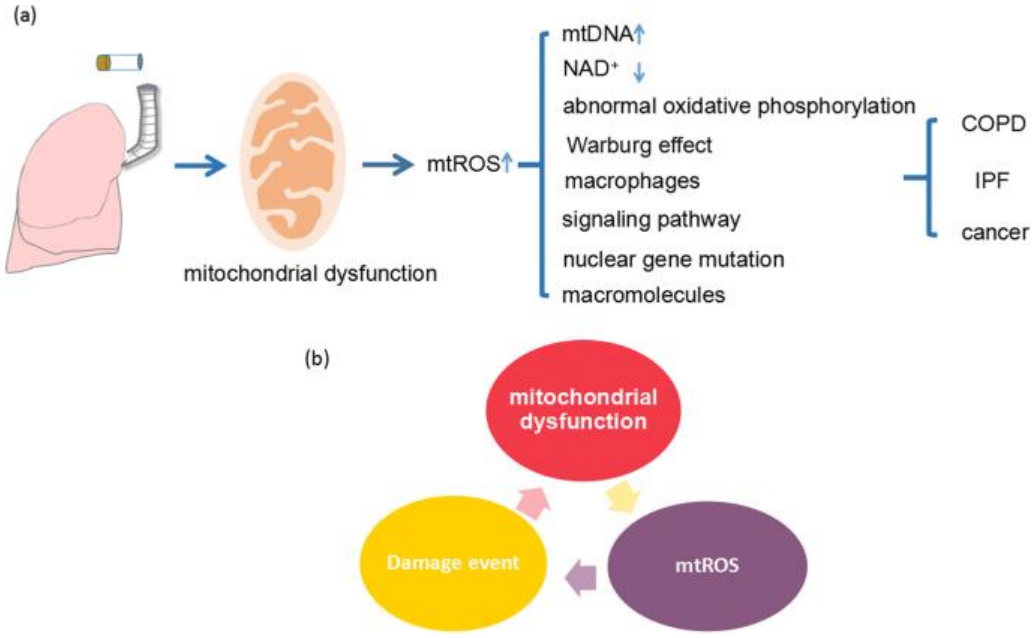

Figure 2.8: The effects of mitochondrial dysfunction on the lungs (Fang *et al*., 2019).

Chapter 3: Materials and Methods

3.1 Materials

FB1 was purchased from Sigma-Aldrich (St. Louis, MO, USA). Equipment and reagents for conducting the Western blot assay were procured from Bio-Rad (Hercules, CA, USA). Antibodies were sourced from Abcam (Cambridge, UK), Sigma-Aldrich (St. Louis, MO, USA), and Cell Signalling Technology (Danvers, MA, USA). All remaining reagents used in this study were acquired from Merck (Darmstadt, Germany), unless indicated otherwise .

3.2 Animal treatment

This study utilised C57BL/6 male mice, approximately 6-8 weeks old, procured from the African Health Research Institute at the University of KwaZulu-Natal (KZN) (Durban, South Africa). The housing conditions for the mice were in alignment with the ARRIVE guidelines and adhered to the protocols outlined by the Animal Research Ethics Committee at the University of KZN (Reference number: AREC/079/016). A random allocation process was employed to categorise the mice into two groups: control and FB1. Each group included five mice, with an average body weight of 20 ± 2.99 g (Figure 3.1). The mice were kept in typical laboratory settings (25°C, 40%-60% humidity levels, 12-hours light/dark cycle). The mice were fed a typical mice pellet diet and had normal drinking water available to them at all times during the study. After a week of acclimatisation, the mice were orally given either 5 mg/kg FB1 solution (FB1 group) or 0.1 M PBS (Control group) for 24 hours. The mice were subsequently euthanised humanely with halothane anaesthesia, and their lungs were harvested for analysis. The lungs were washed three times with 0.1 M PBS and were then stored in 500 µL of Cytobuster reagent (Novagen, CA, USA) for protein isolation and 500 µL of Qiazol reagent (Qiagen, 79306) for RNA extraction and 0.1 M PBS to measure lipid peroxidation levels. All samples were stored (-80°C) until later processing.

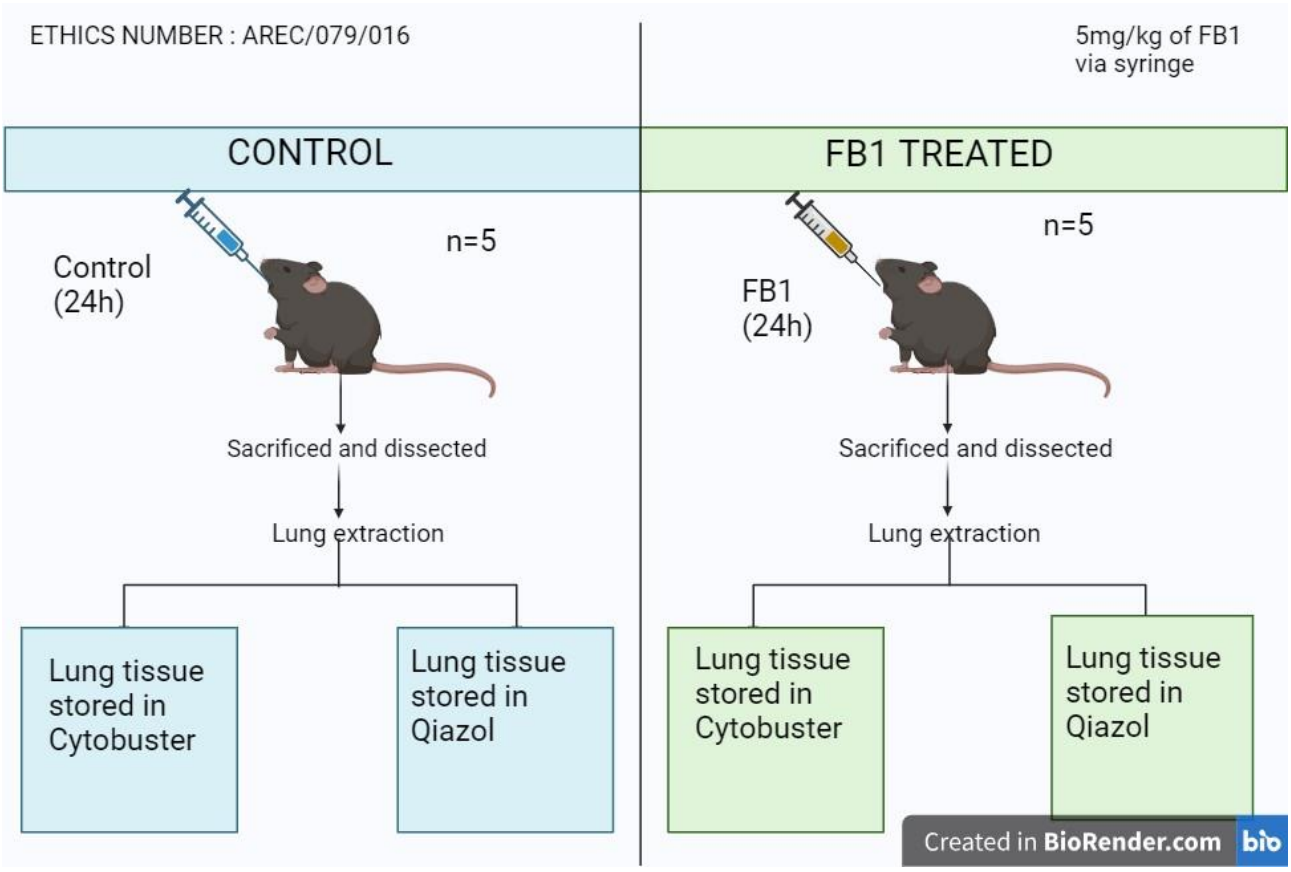

Figure 3.1: Mice treatment and lung extraction (prepared by author).

Sample preparation - homogenisation.

The lungs stored in Cytobuster, Qiazol and PBS reagents were allowed to thaw on ice. Subsequently, the samples were homogenised using a mechanical homogeniser. The resulting homogenates were transferred into microcentrifuge tubes and centrifuged (10 000 xg, 4ºC, 10 minutes (mins)). The appropriate supernatants for the extraction of RNA, protein, and serum were retained for additional analysis through qPCR, western blotting, and the TBARS assay, respectively.

3.3 Quantitative polymerase chain reaction (qPCR)

The quantitative polymerase chain reaction (qPCR) is for the amplification of DNA sequences through a series of enzymatic reactions and is utilised as a diagnostic instrument for assessing genetic integrity, detecting infections, and determining genetic variations (Steward, 2022). The qPCR experiment involves the replication of a DNA molecule in multiple iterations, resulting in a chain reaction. For the reaction to proceed the procedure requires a combination of DNA template, DNA polymerase, primers, and nucleotides. The synthesis of complementary DNA (cDNA) strands is aided by the thermostable Taq polymerase enzyme, which incorporates Deoxynucleoside triphosphates (dNTPs) into the oligonucleoside primers. These primers are complementary to the target gene and flank the target gene. A thermocycler is employed during the qPCR experiment and involves a series of repetitive cycles of three incubation steps, which are conducted at varying temperatures.

The qPCR protocol comprises of three sequential steps: denaturation, annealing, and extension (Figure 3.2). Denaturation is the initial step and allows for the unwinding of the double helix configuration of the DNA molecule. This occurs due to the disruption of hydrogen bonds within the DNA, achieved by exposing the samples to a temperature of 90ºC. The annealing step promotes the formation of complementary base pairs within a temperature range of 45 ºC to 65 ºC. The extension step plays a role in generating a new DNA strand that is complementary to the original template. This is accomplished through the activity of the DNA polymerase enzyme, which operates most effectively at a temperature of 72ºC.

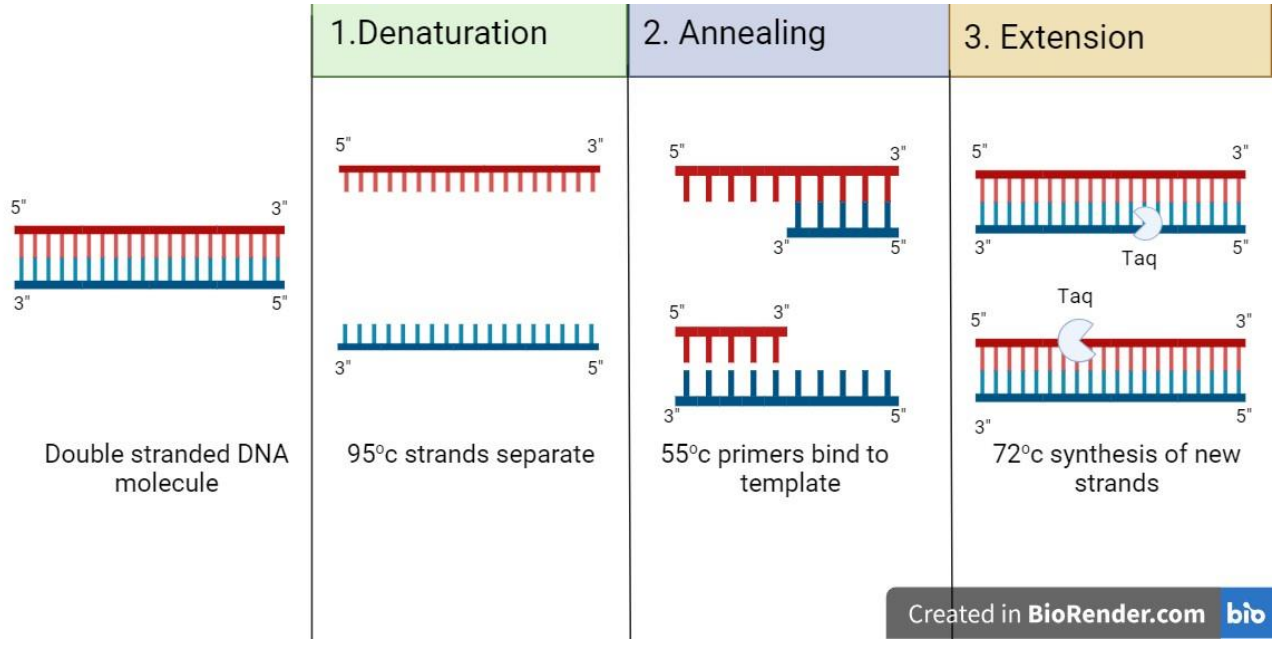

Figure 3.2: A representation of the three stages that form a single cycle of PCR, which is utilised in the amplification of DNA (prepared by author).

This study applied the above qPCR principles to quantify the amount of DNA produced during each cycle of the PCR process. The presence of amplicons was identified by using a DNA-intercalating dye SYBR® Green that emits strong fluorescence upon attachment to the minor grooves of the double-stranded DNA (Figure 3.3). The double-stranded DNA present is directly proportional to the intensity of the fluorescence.

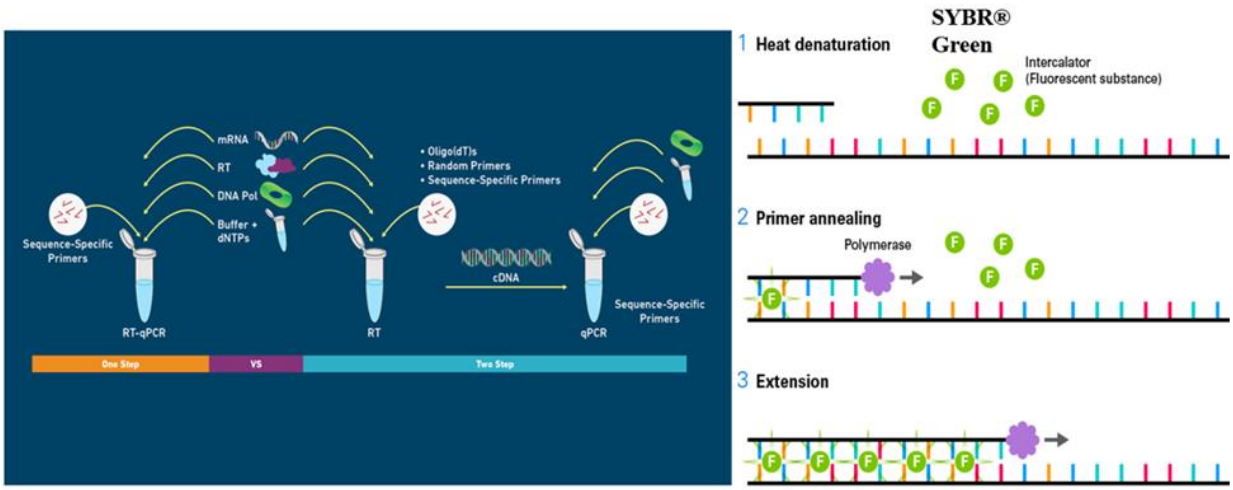

Figure 3.3: qPCR procedure (Steward, 2022).

Necessary regents for the PCR procedure:

- DNA template - Contains the desired sequence.
- Forward and reverse primers - Attaches to the 3' end of the forward and reverse strands of the desired sequence.
- Taq polymerase - Adds nucleotides to the ends of the annealed primers to facilitate the synthesis of new strands that are complementary to the target sequence.
- Deoxynucleoside triphosphate (dNTPs) - building blocks necessary for the construction of new DNA strands.
- $MgCl_2$ - A Taq polymerase co-factor that aids in stabilizing the DNA strands and ensures optimal functioning of the Taq polymerase.
- Buffer system - maintains the optimal pH required for the PCR reaction.

3.3.1 RNA isolation and quantification

RNA was extracted from homogenised tissue samples of the control and FB1 (24 hours) groups, which had been stored in Qiazol. Thawing of the samples was performed at RT. Once thawed, chloroform (100 µL) was added to each sample and centrifuged (4ºC, 12,000xg, 15 mins). The crude RNA present in the aqueous phase was transferred into fresh microcentrifuge tubes. Isopropanol (250 µL) was introduced to each tube and the samples were then centrifuged to form RNA pellets. The pellets were rinsed with 75% ethanol (500 µL) and subjected to another round of centrifugation (7,400xg, 15 mins, 40ºC). Once centrifuged, the ethanol was discarded, and the pellets were permitted to air dry (≈ 30 mins). Once dry the pellets were re-suspended using nuclease-free water (15 µL). Following this, RNA quantification was carried out using the Nanodrop2000 spectrophotometer (Thermo-Fisher Scientific), and the samples were adjusted to a concentration of 300 ng/µL.

3.3.2 cDNA synthesis

The cDNA Synthesis Kit (K1652, Thermo-Fisher Scientific, Waltham, MA, USA) was used to synthesize cDNA in accordance with the manufacturer's instructions. A reaction volume was prepared, which included Oligo$(dT)_{18}$ primer (25 pmol) (0,25 µL), 10mM dNTP mix (1 µL), and nuclease-free water (12,75 µL). The mastermix (14 µL) was added into mini microcentrifuge tubes, the template RNA (1 µL) was added directly to the tubes. The samples were then incubated using the thermocycler (65°C, 5 mins). Thereafter the samples were left to cool down and a second master mix was prepared, which included 5x RT Buffer (4 µL) and Maxima H Minus enzyme mix (1µL). The master mix (5µL) was added to each microcentrifuge tube. The thermocycler was programmed with the following parameters: 10 mins at 25°C, followed by 15 mins at 50°C, and the reaction was terminated by heating at 85°C for 5 mins. Finally, nuclease-free water (60 µL) was added to each sample.

3.3.3 Gene expression

Gene expression analysis was conducted using SYBR® Green Supermix (A25742, Thermo-Fisher Scientific, Waltham, MA, USA). The study utilised forward and reverse primers to investigate the expression of genes linked to oxidative stress (*SOD1*, *SOD2*, *CAT*, *Gpx*, *Nrf2*), in addition to genes involved in mitochondrial dynamics and mitophagy (*Parkin*, *Pink 1*, *p62*, *Sirt3* and *Lonp1*), as well and DNA methylation related genes (*MBD2*, *DNMT3A*, *DNMT3B* and *DNMT1*) (Table 3.1). The housekeeping gene GAPDH was employed to normalize the individual mRNA expression levels. A master mix was prepared by combining the following reaction volumes required per well: SYBR green (5 µL) forward primer (1 µL), reverse primer (1 µL), nuclease-free water (2 µL). The master mix was dispensed into the appropriate wells, and the cDNA (1 µL) from the samples was pipetted in triplicates within the corresponding wells.

The Quant Studio 3 real-time PCR system was used to amplify the genes of interest. Each gene of interest was subjected to the following steps: Initial denaturation (95ºC, 8 mins), followed by denaturation (15 seconds (sec), 95ºC) consisting of 40 cycles, annealing (40 sec, temperatures listed in Table 3.1), and extension (30 sec, 72ºC). The expression levels of the genes of interest were normalized in relation to the housekeeping gene, GAPDH, which underwent simultaneous amplification under the same experimental conditions. The results were represented as a fold-change relative to the control after analysis using the Livak and Schmittgen ($2^{-\Delta\Delta Ct}$) method (Livak and Schmittgen, 2001).

Table 3.1: Temperatures and annealing sequences of genes of interest.

Genes	Annealing Temperatures	Primer	Sequences
SOD1	60^{o}C	Forward Reverse	5'TATGGGGACAATACACAAGGCT 3' 5'CGGGCCACCATGTTTCTTAGA3'
SOD2	60^{o}C	Forward Reverse	5'GGCATCTTGTTGGGAATGTG 3' 5'AGACCTGCCTTACGACTATGG3'
CAT	60^{o}C	Forward Reverse	5'TGGCACTTTGACAGAGAGC 3' 5'CTTTGCCTTGGAGTATCTGG 3'
Gpx	58^{o}C	Forward Reverse	5'AGTCCACCGTGTATGCCTTCT 3' 5'GAGACGCGACATTCTCAATGA3'
Nrf2	58^{o}C	Forward Reverse	5'CTTTAGTCACCGACAGAAGGAC3' 5'AGGCATCTTGTTTGGGAATGTG3'
Sirt3	60^{o}C	Forward Reverse	5'TACAGGCCCAATGTCACTTCA 3' 5'ACAGACCGTGCATGTAGCTG 3'
Lonp1	60^{o}C	Forward Reverse	5'CTCATGGTGGAGGTTGAGAATG3' 5'CAGAGGGTTCAAGGCGATGAT3'
Parkin	60^{o}C	Forward Reverse	5'TCCTTCGTCCACTGTTTCACA3' 5'GGGCATTGCTCTCAGTCACAT3'
Pink1	60^{o}C	Forward Reverse	5' CCACTGTTCCTCGTTATGAAGA3' 5'TCCGCTAGTTGAACATACAGGAT3'

p62	60°C	Forward Reverse	5’ CCTCTGAGTCTCGGGAATTTCA3’ 5’ GACTTACTGCACGTTTGGGC3’
DNMT3A	60°C	Forward Reverse	5’GGCCGAATTTCTTGGTG3’ 5’CCATCTCCGAACCACACATGAC3’
DNMT3B	60°C	Forward Reverse	5’AGCCGCGTATGAGGAGTGCAT3’ 5’GGGAGCATCCTTCGTGTCTGG3’
DNMT1	60°C	Forward Reverse	5’AGAGACCAGGATAAGAAACGCA3’ 5’CTCCTTTGATTTCCGCCTCAAT3’
MBD2	58°C	Forward Reverse	5’ACTTCACCRRATTGCTCGGGT3’ 5’AGAACAAGGGTAAAGGAGACCT3’
GAPDH	House keeping	Forward Reverse	5’TCCACCACCCTGTTGCTGTA3’ 5’ACCACAGTCCATGCCATCAC3’

3.4 Western blotting

The western blotting procedure begins with the separation of proteins according to their molecular weight, using electrical fields (Gavini and Parameshwaran, 2025). Thereafter, the proteins are transferred to a solid surface for detection, where they are probed using antibodies to generate bands (Figure 3.4). the density of these bands is directly proportional to the amount of protein of interest being expressed. The western blotting technique allows for the detection and quantification of target proteins within a sample that comprises of various other proteins.

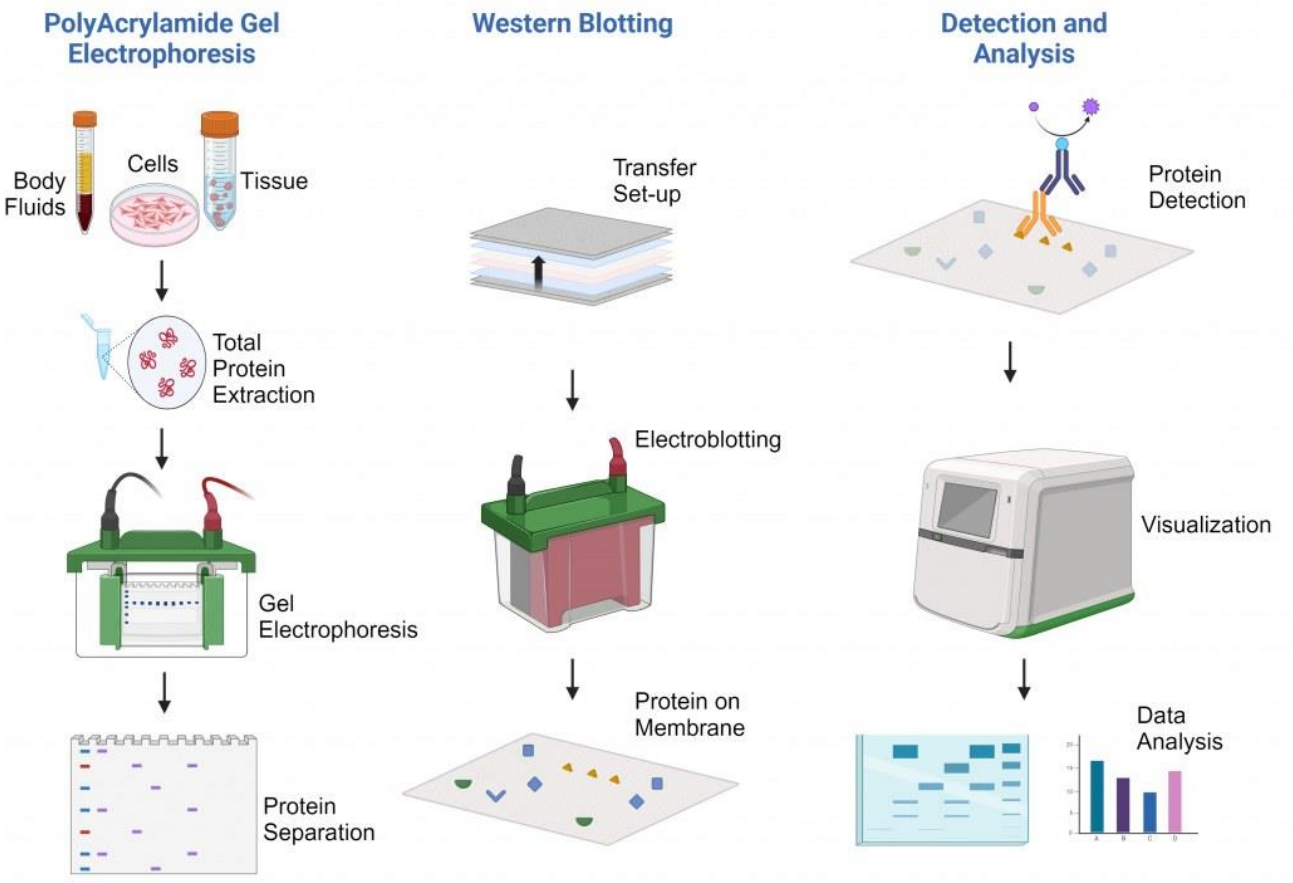

Figure 3.4: Image representing the steps performed during the western blotting procedure (Clinisciences, 2024)

3.4.1 Protein isolation and protein preparation

The crude protein was extracted from the mouse lung tissue through the application of Cytobuster™ Protein Extraction Reagent (catalogue no. 71009, Novagen, Bloemfontein, SA). When used in conjunction with homogenisation the non-ionic detergent Cytobuster facilitates effective extraction of soluble and functionally active proteins. To mitigate protein degradation and impairment caused by the release of proteases and phosphates from cells during the process of protein isolation, a mixture of protease and phosphate inhibitors is added into the Cytobuster lysis reagent.

3.4.2 Protein quantification and standardization

The determination of protein concentration in the samples is achieved through the bicinchoninic acid (BCA) assay. The purpose of this assay is to validate the presence of sufficient protein and to enable alterations in the protein concentration of the samples, ensuring that protein levels are consistent across all samples (Proteomics, 2024). The BCA assay is primarily based on the biuret reaction, where cupric ions (Cu^{2+}) are reduced to cuprous ions (Cu^{+}) by peptide bonds. Following this, the Cu^{+} react with two molecules of BCA to form a BCA-Cu^{+} complex, which appears as an intense purple colour. Which is measured using a spectrophotometer at a wavelength of 562 nm. The colour intensity produced is directly correlated to the concentration of proteins present in a sample. Thus, the protein content within a sample can be quantified by employing the BCA assay as a reliable indicator.

Standards of bovine serum albumin (BSA) concentrations [0, 0.2, 0.4, 0.6, 0.8, and 1 mg/mL] were prepared using distilled water. After preparing the standards, a 96-well microtiter plate was used to plate each standard in triplicate and each protein in duplicate. Each well then received 40 µL of working solution, that was made up by combining BCA (39,6 µL per a well) and $CuSO_4$ (0,8 µL per a well). The plate then underwent an incubation period (37ºC, 30 mins). Following incubation, the absorbance was read at 562 nm using the SPECTROstar® Nano microplate reader (BMG LABTECH, Ortenberg, Germany). After standardisation of the proteins to 1 mg/mL using Cytobuster, Laemmli buffer was dispensed into each sample and then subjected to boiling (5 mins, 100ºC).

Components making up Laemmli buffer and their functions:

- Glycerol - enhances the sample viscosity enabling it to sink to the bottom of the well.
- 10% Sodium dodecyl sulphate (SDS) - imparts a uniform negative charge to the sample and guarantees protein sample linearization.
- 0,5 Tris - maintains the sample pH level.
- 5% β-mercaptoethanol - enhances linearity in proteins by breaking down disulfide bridges and bonds.
- 1% bromophenol blue - serves as a protein tracking dye in the process of electrophoresis.

3.4.3 Preparation of SDS-PAGE

The sodium dodecyl sulphate polyacrylamide gel electrophoresis (SDS-PAGE) technique is employed to separate proteins, to allow for the assessment of individual protein expression. SDS-PAGE enables charged molecules to traverse a gel matrix when an electric current is applied (Nowakowski *et al.*, 2014).

Polyacrylamide gels are characterised as three dimensional-polymers created from acrylamide and the cross-linker N,N'-methylene bis-acrylamide, with ammonium persulfate (APS) acting as the catalyst for the formation (Nowakowski *et al*., 2014). SDS-PAGE utilises 2 variants of agarose gels to facilitate the differentiation of proteins according to their molecular weights. The stacking gel which constitutes the upper portion of the gel system is slightly acidic (6.8 pH) in nature and is characterised by its large pores that do not separate proteins because of its low polyacrylamide concentration. However, it plays a crucial role in enabling proteins to develop thin, distinctly defined bands. which are subsequently separated in the lower resolving gel. The resolving gel has a basic pH (pH 8.8) and is distinguished by a high polyacrylamide concentration along with narrow pore structures, which facilitates the separation of proteins according to their molecular weight.

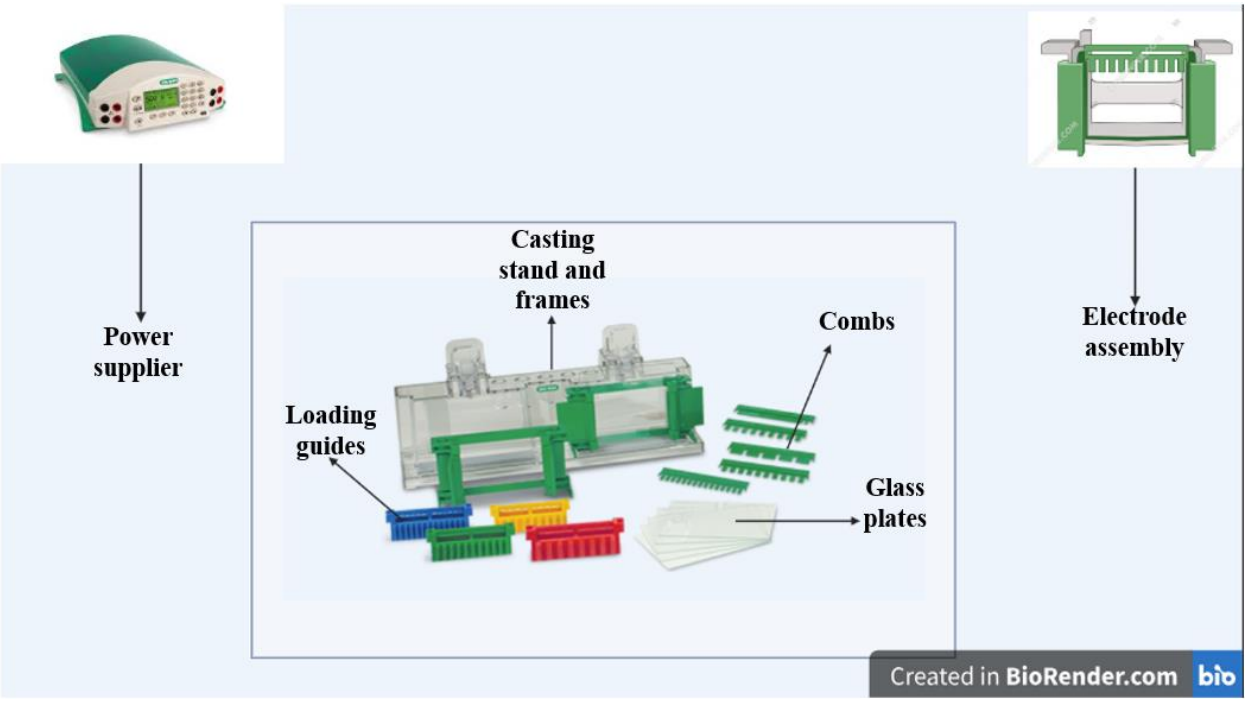

Figure 3.5: SDS-PAGE equipment required for gel preparation (created by author).

The gels for SDS-PAGE were made utilising the Mini-PROTEIN Tetra cell casting stands (Bio-Rad) (Figure 3.5).The components for the 10% resolving gel [dH_2O, 1.5 M Tris (pH 8.8), 10% SDS, bis-acrylamide, 10% APS and TEMED] were combined and the mixture was then allowed to set for a period of 1 hour. This was succeeded by formulation and addition of 4% stacking gel [dH_2O, 0.5 M Tris (pH 6.8), 10% SDS, bis-acrylamide, 10% APS and TEMED]. A 1.5 mm plastic comb was inserted between the glass plates to establish wells for loading, and the gels were allowed to undergo polymerization for roughly 45 mins.

SDS-PAGE

The gel cassettes were then inserted into the electrode tank of the Mini-PROTEIN Tetra cell system (Bio-Rad), and the tank was filled with 1X running buffer [25mM Tris, 192mM glycine and 0.1% SDS]. The wells were subsequently filled with 25 µL of protein samples, which were then subjected to electrophoresis (150V, 1.5 hours).

3.4.4 Protein transfer

The gels were separated from the glass plates, and the stacking gel was discarded, while the resolving gel was retained. Transfer buffer [25 mM Tris, 192 mM glycine and 20% methanol (pH 8.3)] was used to equilibrate the resolving gel, the nitrocellulose membrane, and two fibre pads. Once equilibration was achieved, a layered arrangement of a fibre pad, nitrocellulose membrane, gel, and another fibre pad were inserted into the transfer cassette. Trans-Blot Turbo Transfer System was used to transfer the separated proteins to a nitrocellulose membrane (30 mins, 25V; Bio-Rad). The application of the voltage allows the negatively charged proteins to move from the gel to the nitrocellulose membrane. The electric current being produced is oriented at a right angle to the gel's surface.

3.4.5 Blocking and antibody incubation

To mitigate non-specific protein binding after the transfer, the membranes were incubated (1 hour, RT) with 5% BSA in Tris buffered saline containing 0.05% Tween 20 [150 mM NaCl, 3 mM KCl, 25 mM Tris, 0.05% Tween 20, dH_2O (pH 7.5)]. They were then probed with the specific primary antibodies (Table 3.2) for 10 mins on the shaker, then left to incubate overnight (4^{o}C). After the overnight incubation, the membranes were allowed to acclimate to RT. To ensure the complete removal of any unbound primary antibody, the membranes underwent five washes with TTBS. They were then probed with the specified horse-radish peroxidase (HRP)-conjugated secondary antibody (Table 3.2) for a duration of 1 hour at RT, with continuous gentle agitation. The unique characteristics of the secondary antibody enable it to exclusively link to the primary antibody of interest. Upon completion of the incubation, the membranes underwent five washes (10 mins, RT) with TTBS to ensure the removal of any unbound secondary antibodies.

3.4.6 Imaging

The visualization of the antigen-antibody complex was achieved using the Clarity™ Western ECL Substrate Kit (catalogue no. #170-5060, Bio-Rad) which includes a hydrogen peroxide substrate along with an improved luminol solution. The HRP conjugated to the secondary antibody reacts with the H_2O_2 substrate, leading to the formation of oxygen radicals. These radicals subsequently degrade luminol into aminophthalic acid. The aminophthalic acid then reacts with enhancer molecules, resulting in luminescence that enables the visualization of protein bands. The Invitrogen iBright imaging system (Thermo-Fisher Scientific) was used to visualize the protein bands. This apparatus features a camera-based imaging mechanism that recognizes the chemiluminescent signals emitted.

To facilitate band detection, 250 µL of the Clarity Western ECL Substrate detection reagent (Bio-Rad) was introduced to the membranes, images were subsequently captured with an Invitrogen iBright imaging system (Thermo-Fisher scientific).

3.4.7 Quenching and normalizing

After the detection phase, the membranes underwent a quenching process with 5 mL of H_2O_2 (30 mins, 37°C). Following this, the membranes underwent a single wash with TTBS (10 mins, RT). Subsequently, a blocking procedure was conducted using 5% BSA in TTBS (1 hour, RT). For a period of 30 mins at RT, the probing step was undertaken with the house keeping protein β-actin (Table 3.2). To ensure precise measurement of protein levels, a housekeeping protein was utilised for the normalization of protein expression. These proteins act as internal reference points, consistently expressed to mitigate errors that may arise from variations in loading and protein standardisation.

The analysis of protein expression was conducted using iBright^{TM} analysis software (Thermo-Fisher Scientific), with the results quantified as percentage (%) fold-change and band density.

Table 3.2: Antibodies and antibody dilutions.

Primary Antibody	Secondary Antibody	Catalogue number
Anti-SOD2 (1:1000 in 5% BSA)	Anti-Rabbit (1: 1000 in 5% BSA)	Cell Signaling Technology, #3286
Anti-CAT (1: 1000 in 5% BSA)	Anti-Rabbit (1: 1000 in 5% BSA)	Cell Signaling Technology, #12980
Anti-Sirt3 (1: 1000 in 5% BSA)	Anti-Rabbit (1: 1000 in 5% BSA)	Abcam, ab86671
Anti-Lonp1 (1: 1000 in 5% BSA)	Anti-Rabbit (1: 1000 in 5% BSA)	Sigma- Aldrich, HPA002192
Anti-parkin (1: 1000 in 5% BSA)	Anti-Mouse (1 in 5000 in 5% BSA)	Abcam, ab77924
β-actin (1: 1000 in 5% BSA)	House keeping	Merck, A3854

3.5 DNA Methylation ELISA

Enzyme-linked immunosorbent assay, abbreviated as ELISA, is a diagnostic approach employed to detect antigens in biological samples. Like other immunoassay techniques, ELISA utilizes antibodies to recognize a specific target antigen through highly selective antibody-antigen interactions (Figure 3.6) (Alhajj *et al*., 2023). The ELISA assay utilizes a polystyrene microtiter plate, as its polystyrene properties increase the ability of proteins to adhere to the wells. The wells of the polystyrene plate are coated with the relevant antigen. The DNA methylation ELISA is a colorimetric assay consisting of three steps. Step 1 involves DNA binding to the wells of the plate. This is followed by the methylated DNA capture step which involves the detection of DNA through the addition of capture and detection antibodies, as wells an enhancer solution. The final step is known as signal detection and involves the addition of developer solution. Once a blue colour change occurs, the reaction is typically stopped using stop solution. A spectrophotometer can be utilized to measure the absorbance of the colour change produced. The readings obtained can then be used to generate a standard curve to calculate the concentrations of the relevant proteins (abcam, 2024).

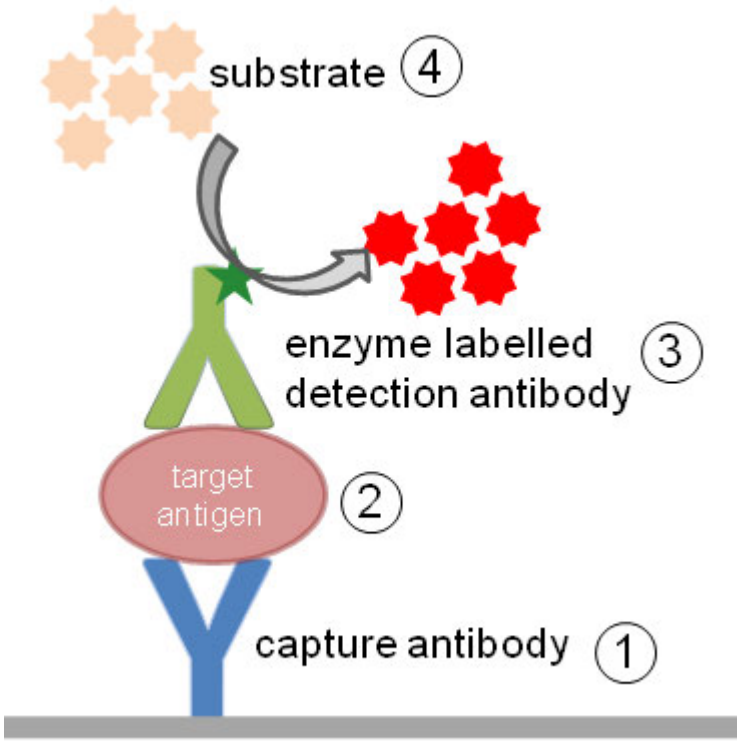

.

Figure 3.6: The ELISA principle (Horlock, 2016)

3.5.1 DNA isolation and quantification

DNA was isolated from homogenised tissue samples from both the control and FB1 (24 hours) groups, which had been stored in Qiazol. The DNA isolation procedure is made up of three phases. The first phase of this procedure involved precipitating the DNA. This process began with the elimination of any remaining aqueous phase that was present above the interphase. Following this, 100% ethanol (150 µL) was introduced to the samples. After mixing the samples by inverting the microcentrifuge tubes, they were incubated for 2 to 3 mins. Following the incubation period, the samples underwent centrifugation (5 mins, 2000xg,4ºC) to yield a DNA pellet. The phenol-ethanol supernatant was then moved to a new microcentrifuge tube and subsequently stored. In the second phase of this protocol, the DNA pellet was subjected to a washing procedure. The initial step involved resuspending the pellet in 0.1 M sodium citrate in ethanol (500 µL) (pH 11.5). The resuspended DNA pellet was then incubated for a duration of 30 mins, during which it was mixed intermittently by inverting the microcentrifuge tube. Following this incubation, the pellet was centrifuged (5 mins, 2000xg,4ºC) once more, and the resulting supernatant was subsequently discarded. The DNA pellets were later suspended in a 75% ethanol solution (100 µL) and incubated for 10 to 20 mins, with gentle inversion performed intermittently. Following the incubation period, the DNA pellets were centrifuged (5 mins, 2000xg, 4ºC), the supernatant was discarded, and the pellets were left to air dry. The third phase of this procedure involved the solubilisation of the DNA pellet. The pellet was first resuspended in 8 mM NaOH and then subjected to centrifugation to eliminate insoluble materials. Subsequently, the supernatant was pipetted into new microcentrifuge tubes, where the pH was adjusted using HEPES buffer. The DNA was then quantified using the Nanodrop2000 spectrophotometer (Thermo-Fisher Scientific) (Ghazi, 2019).

3.5.2 Global DNA Methylation ELISA

Necessary regents for the procedure

- 1X wash buffer - add 10X wash buffer to dH_2O (117 mL).
- Positive control - dilute positive control to 10 ng/µL (5 µL of positive control + 3 µL of 1X TE buffer).
- Dilute capture antibody - add capture antibody to diluted wash buffer (1:1000 dilution).
- Dilute detection antibody- add detection antibody to diluted wash buffer (1:2000 dilution).
- Dilute enhancer antibody - add enhancer antibody to diluted wash buffer (1:1000 dilution).
- Developer solution.
- Stop solution.

The process began with creating five varying concentrations using the 10ng/µL diluted positive control and 1x TE buffer [0,5; 1; 2; 5 and 10 ng/µL), according to the outlined dilution chart.

A colorimetric DNA methylation quantification kit (Abcam, ab117128) was utilised to measure DNA methylation levels, in accordance with the manufacturer's specifications. The assay was divided into three phases. The first phase focused on DNA binding, where the necessary number of strip wells was determined, and the excess wells were removed. Binding solution (80 µL) was then pipetted into each well. The next step involved the introduction of the negative control (1 µL), diluted positive control (1 µL) as well as the mice lung tissue control and FB1 samples (8 µL) into their designated wells. The solution was mixed by gently tilting the plate to achieve uniform coverage. The strip plate was subsequently sealed with parafilm and allowed to incubate (90 mins, 37^{o}C). Once incubation had concluded, the binding solution was discarded from each well, and was subjected to three washes with 1X wash buffer (150 µL). The second phase of the procedure focused on the capture of methylated DNA. To begin, a diluted capture antibody was introduced to each well (50 µL). The plate was subsequently enclosed and subjected to incubation conditions. After the incubation phase, the diluted capture solution was taken out, and the wells were rinsed three times with a diluted wash buffer (150 µL). Next, a diluted detection antibody was introduced into each well. The plate was covered once more and incubated (60 mins, RT). Once the incubation concluded, the diluted detection antibody was discarded, and the wells were rinsed four times with the diluted wash buffer (150 µL). Following the addition of the dilute enhancement solution (50 µL) to each well, the plate was sealed and incubated (30 mins, RT). After the incubation period concluded, the dilute enhancement solution was removed, and the wells were subjected to five washes with a diluted wash buffer (150 µL). The third and final phase focused on signal detection. Development solution (50 µL) was first introduced to the wells, and the plate was incubated (1 to 10 mins) in a dark environment. Thereafter, a stop solution (50 µL) was pipetted into the wells to terminate the enzyme reaction. The plate's absorbance was read at 450 nm with the SPECTROstar® Nano microplate reader (BMG LABTECH, Ortenberg, Germany). The optical density readings obtained was used to construct a standard curve in order to determine the 5-methylcytosine (5-mC) levels present.

3.6 Thiobarbituric Acid Reactive Substances (TBARS) Assay

The mitochondria are a source of free radical production. During ATP production, free radicals are produced, and these have the potential to induce lipid peroxidation. Lipid peroxidation results in the formation of the by-product MDA (Figure 3.7), which can be measured using the TBARS assay. It is a common way to quantify lipid peroxidation products in cells, tissues, and body fluids (De Leon and Borges, 2020). The TBARS assay quantifies the reaction between MDA and Thiobarbituric acid (TBA), which produces a red-pink complex. The degree of colour intensity is proportional to the level of lipid peroxidation in the sample (Figure 3.7).

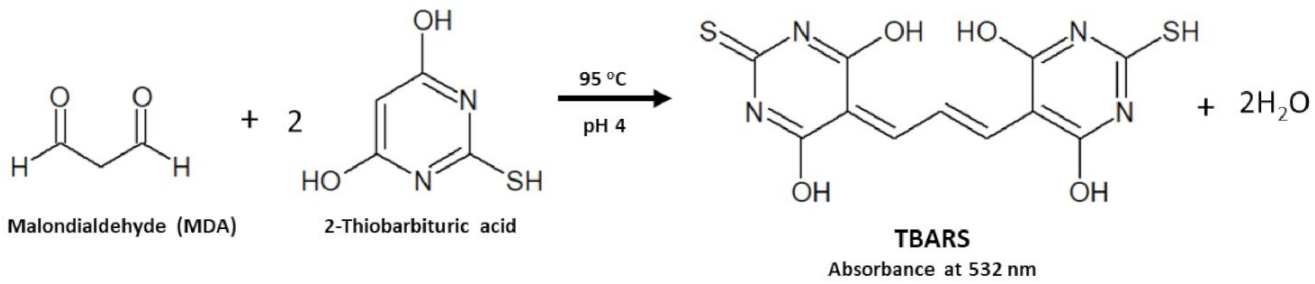

Figure 3.7: Principle of the TBARS assay (De Leon and Borges, 2020)

The homogenised mice lung tissue samples present in PBS (200 µL of control and FB1) were placed in appropriately labelled glass test tubes. Both a negative control and positive control (1 µL MDA) were also made-up. Following this, 7% phosphoric acid (H_3PO_4) (200 µL) was added to each test tube, and TBA-BHT (400 µL) was included in all but the negative control, which received 3 mM hydrochloric acid (HCl) (400 µL). The samples were boiled and then cooled (RT). Next, butanol (1500 µL) was introduced to each sample, and the mixture was vortexed until two distinct phases formed. The upper butanol phase (500 µL) was extracted, and 100 µL was pipetted into a 96-well microtiter plate in triplicate. Absorbance readings were taken at 532 nm, with a reference wavelength of 600 nm, with the SPECTROstar® Nano microplate reader (BMG LABTECH, Ortenberg, Germany). The average MDA concentration (µM) was determined by dividing the mean of the replicates by the absorption coefficient (156mM-1).

3.7 Statistical analysis

The qPCR, western blotting, DNA methylation and TBARS assays were done three independent times. Microsoft Excel and GraphPad Prism version 5.0 (GraphPad Software Inc., California) were utilised for statistical analysis. The unpaired t-test, incorporating Welch's Correction, was applied to all assays. The mean ± standard deviation was used to represent all results, unless specified otherwise. A *p*-value of less than 0.05 was considered statistically significant.

Chapter 4: Results

4.1 Oxidative stress and antioxidant response

4.1.1 TBARS assay

The TBARS assay evaluated the levels of lipid peroxidation in the lung tissue of FB1-treated mice, by measuring the end product of lipid peroxidation (MDA). The results indicated a significant elevation in MDA levels ($p<0.0001$) (Figure 4.1.1) in the lung tissue for the FB1-treated mice relative to the control.

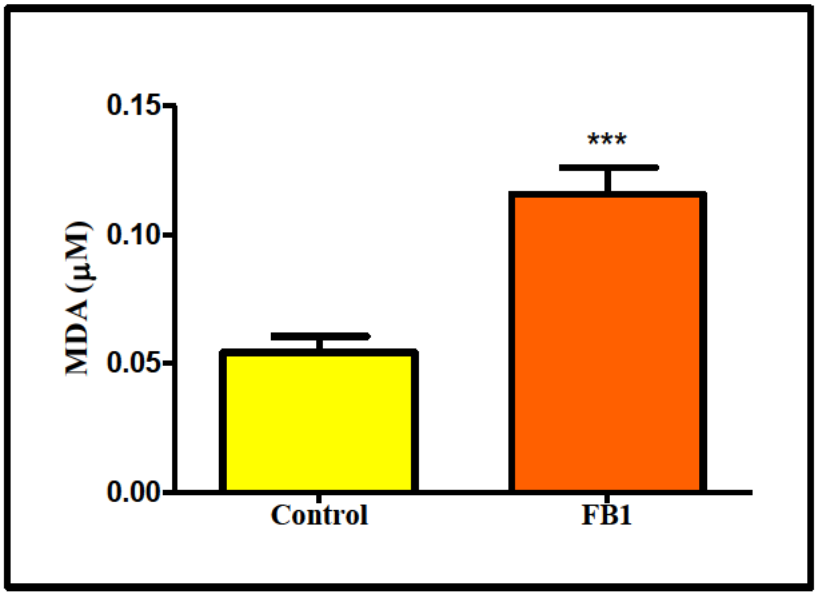

Figure 4.1.1: ROS production in the lung tissue of FB1-treated mice relative to the control. A significant upregulation in MDA levels was present in the lung tissue of FB1-treated mice compared to the untreated control (***$p<0.0001$).

4.1.2 qPCR

Nrf2 is a regulator of essential antioxidant enzymes aimed at mitigating oxidative stress. The gene expression of *Nrf2* in the lung tissue of mice treated with FB1 was significantly reduced (p<0.0001) (Figure 4.1.2 A), which corresponded with the significant downregulation in gene expression of the antioxidants; *SOD1* (p=0.0003) (Figure 4.1.2 B), *CAT* (p<0.0001) (Figure 4.1.2 C), and *Gpx* (p=0.0004) (Figure 4.1.2 D). However, it did not correlate with the non-significant upregulation in *SOD2* (p=0.7454) (Figure 4.1.2 E) levels observed.

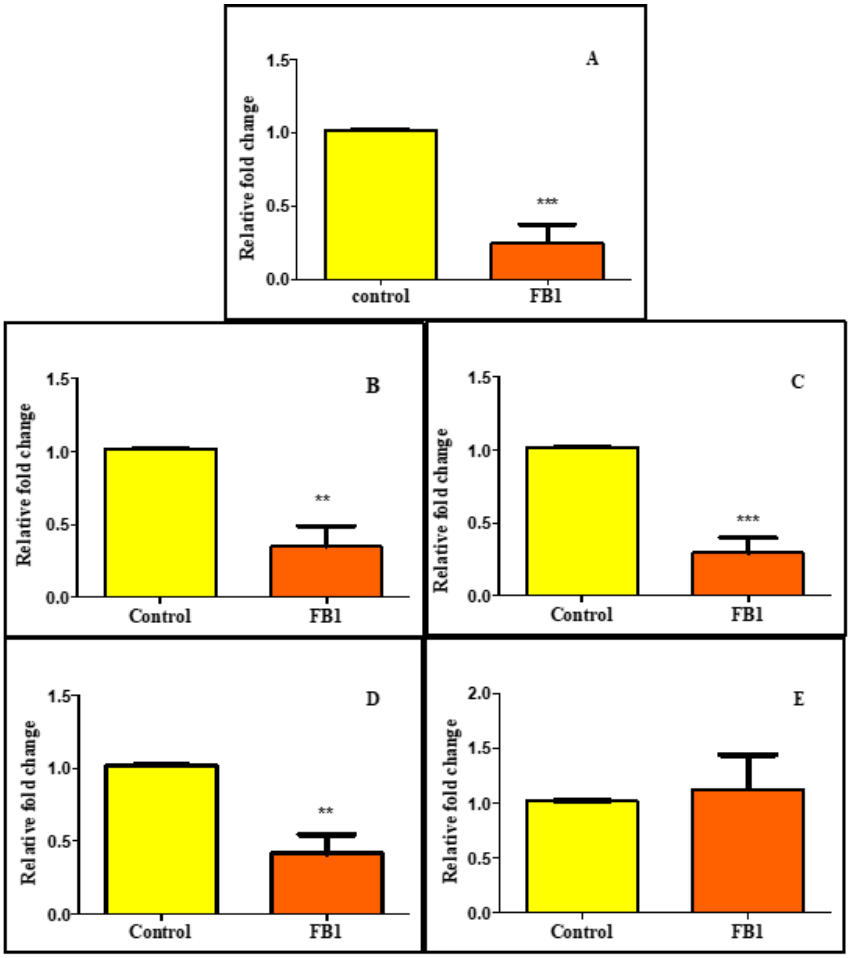

Figure 4.1.2: Antioxidant gene expression in the lung tissue of FB1-treated mice. A significant downregulation in gene expression of (A) *Nrf2,* (B) S*OD1*, (C) *CAT* and (D) *Gpx* present in the lung tissue of FB1-treated mice compared to the control. A non-significant increase in (E) *SOD2* gene expression for the lung tissue of FB1-treated mice in comparison to the control (**p<0.005; ***p<0.0001).

4.1.3 Western Blotting

The lung tissue of FB1-treated mice displayed a non-significant reduction in SOD2 (p=0.7141) (Figure 4.1.3 A) protein levels compared to the control group. A significant decrease in CAT (p<0.0001) (Figure 4.1.3 B) levels was observed in the lung tissue of FB1-treated mice when compared to the control group. These results suggest there is no change in SOD2 to detoxify O_2^- but a reduction in CAT capacity to detoxify H_2O_2.

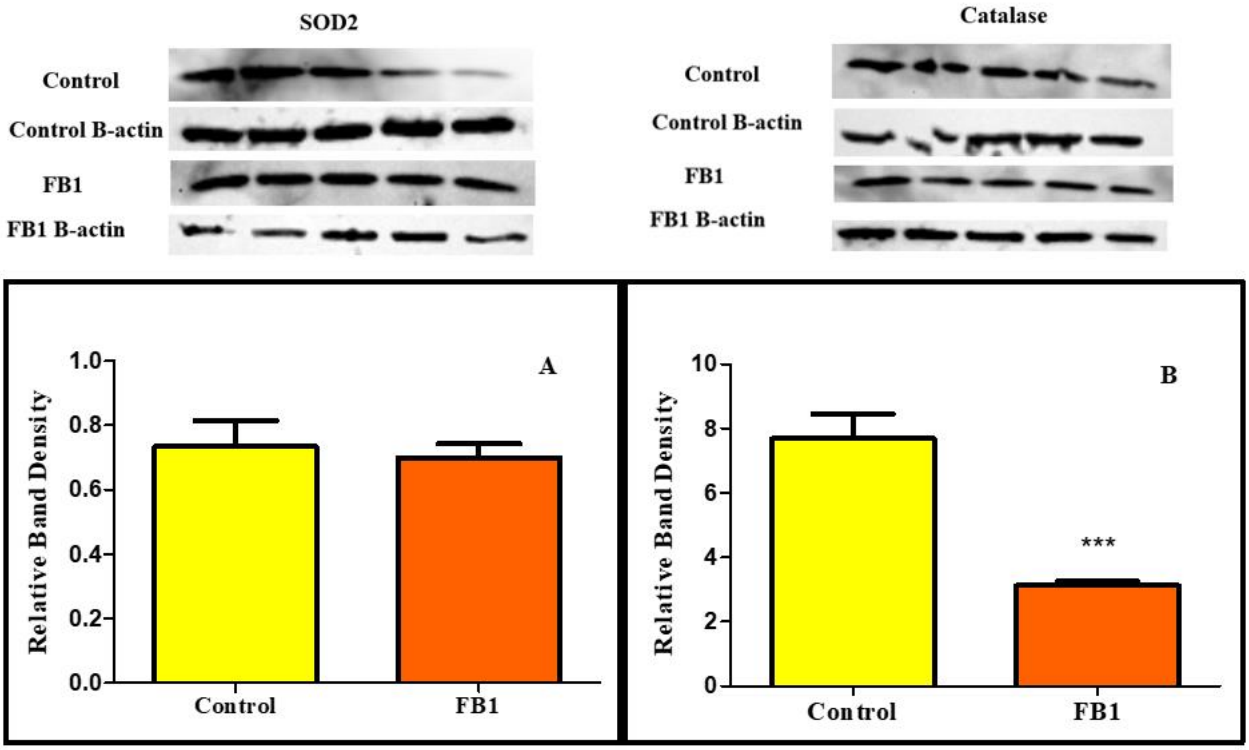

Figure 4.1.3: Antioxidant protein expression in lung tissue of FB1-treated mice compared to the control. A non-significant downregulation in (A) SOD2 levels in the lung tissue of the treated mice relative to the control. A significant downregulation in (B) CAT levels in lung tissue of the FB1-treated mice relative to the control (***p<0.0001).

4.2 Mitochondrial dysfunction and mitophagy

4.2.1 qPCR

Sirt3 and Lonp1 are mitochondrial genes that are upregulated to uphold optimal mitochondrial functionality. A significant increase in *Sirt3* gene expression (p=0.0244) (Figure 4.2.1 A) and a significant downregulation in *Lonp1* gene expression (p<0.0001) (Figure 4.2.1 B) was observed in the lungs of FB1-treated mice. When mitochondrial stress persists, it initiates the process of mitophagy. This activation is primarily driven by the buildup of Pink1 and recruitment of Parkin to the mitochondria. The findings reveal a significant downregulation in *Pink1* gene expression (p<0.0001) (Figure 4.2.1 C) in the lung tissue of FB1-treated mice, which aligns with the downregulation in *Parkin* (p=0.0162) (Figure 4.2.1 D) gene expression. Parkin ubiquitinates various proteins, including p62, to initiate the process of mitophagy. Analysis of lung tissue from FB1-treated mice revealed a significant decrease in *p62* (p<0.0001) (Figure 4.2.1 E) gene expression when compared to the control tissues.

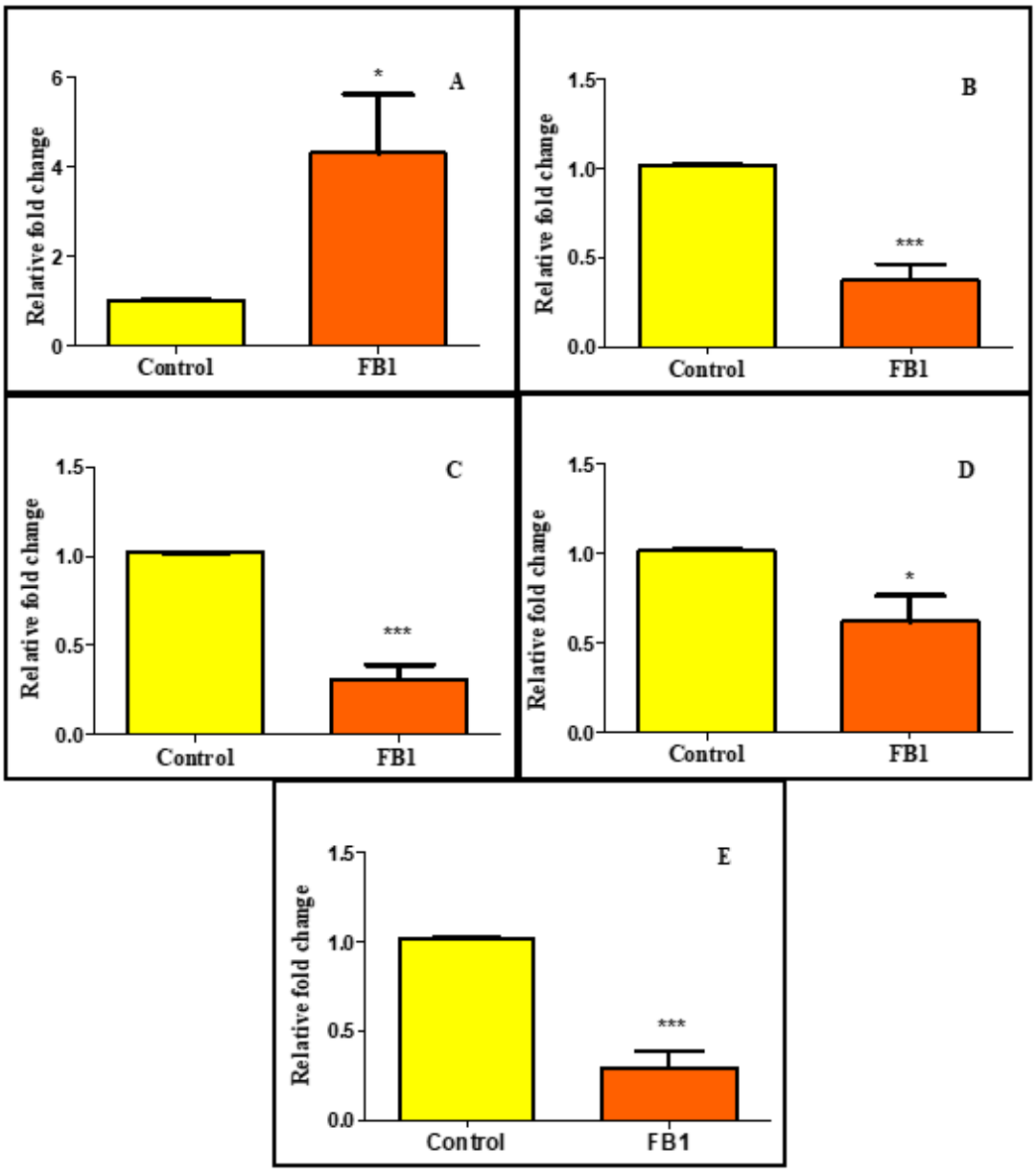

Figure 4.2.1: Expression of mitochondrial dysfunction and mitophagy related gene in lung tissue of the FB1-treated mice compared to the control. A significant upregulation in (A) *Sirt3* and a significant downregulation of (B) *Lonp1* gene expression was present for the lung tissue of the FB1-treated mice. A significant downregulation of (C) *Pink1*, (D) *Parkin*, (E) *p62* was present for the tissue of the treated mice relative to the control (*p<0.05; ***p<0.0001).

4.2.2 Western blotting

A notable increase in Sirt3 (p<0.0001) expression (Figure 4.2.2 A) was present for the lung tissue of the FB1-treated mice. The observed increase corresponds with the significant downregulation in Lonp1 (p<0.0001) (Figure 4.2.2 B) protein expression present for the lung tissue of mice treated with FB1, as Sirt3 is involved in transcriptionally regulating Lonp1 protein expression. The lung tissue of FB1-treated mice exhibited a significant reduction in Parkin (p<0.0001) (Figure 4.2.2 C) protein levels when compared to the control group.

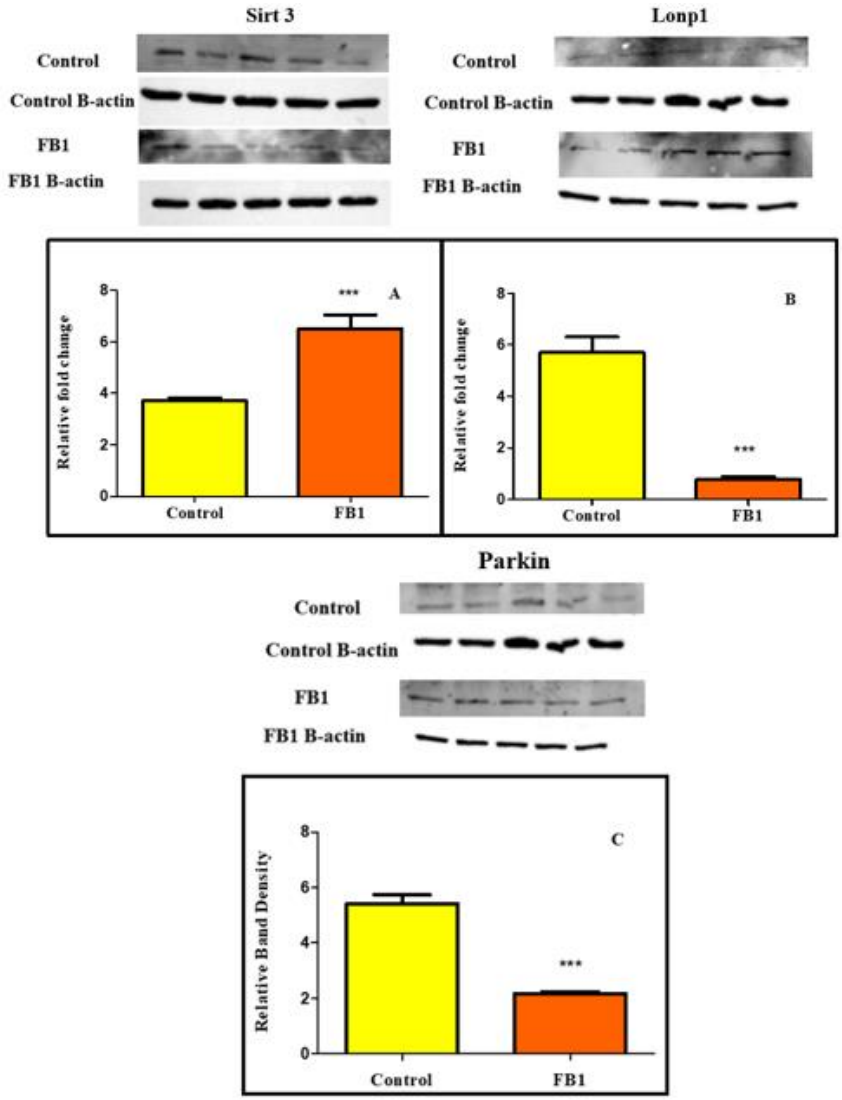

Figure 4.2.2: Expression of mitochondrial dysfunction and mitophagy-related proteins in lung tissue of the FB1-treated mice compared to the control. A significant upregulation in (A) Sirt3 and a significant downregulation of (B) Lonp1 protein expression was observed for the tissue of the treated mice. A significant downregulation of (C) Parkin was observed for the lung tissue of mice treated with FB1 relative to the control (***p<0.0001).

4.3 Global DNA methylation

4.3.1 Global DNA methylation ELISA assay

The level of global DNA methylation in the lung tissue of mice treated with FB1 was measured using ELISA and a significant increase in global DNA methylation levels (p=0.0018) (Figure 4.3.1) was present when compared with the control. FB1 promotes DNA hypermethylation in the mice lungs.

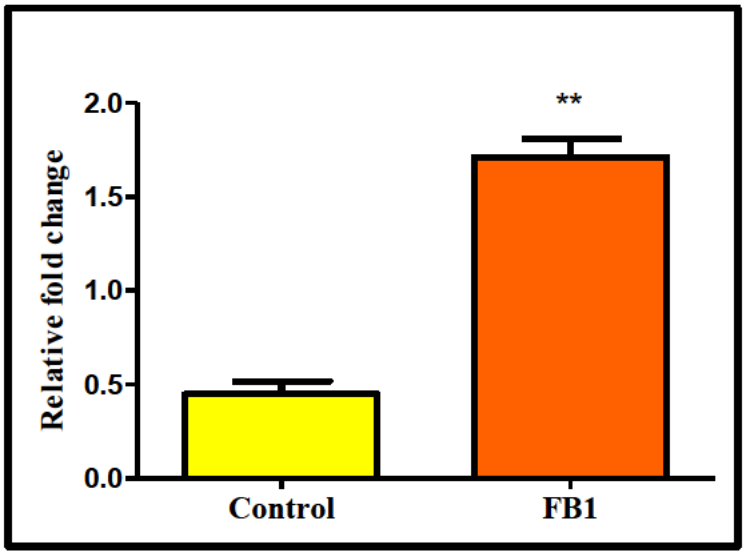

Figure 4.3.1: DNA methylation levels in lung tissue of FB1-treated mice relative to the control. A significant upregulation in global DNA methylation levels was observed in the lung tissue of the FB1-treated mice compared to the untreated control (**p<0.005).

4.3.2 qPCR

Given the hypermethylation of DNA induced by FB1 in the lung tissue of the mice, an assessment of the mRNA expression of the DNMT enzymes was conducted to gain deeper insights into FB1-induced changes in DNA methylation. A significant upregulation in *DNMT3A* (p=0.0082) (Figure 4.3.2 A) and *DNMT3B* (p=0.0047) (Figure 4.3.2 B) as well as a non-significant upregulation in *DNMT1* (p=0.1521) (Figure 4.3.2 C) levels was present in the lungs of the FB1-treated mice relative to the control. A non-significant increase in *MBD2* (p=0.6934) (Figure 4.3.2 D) gene expression was found for lung tissue of the FB1-treated mice relative to the control.

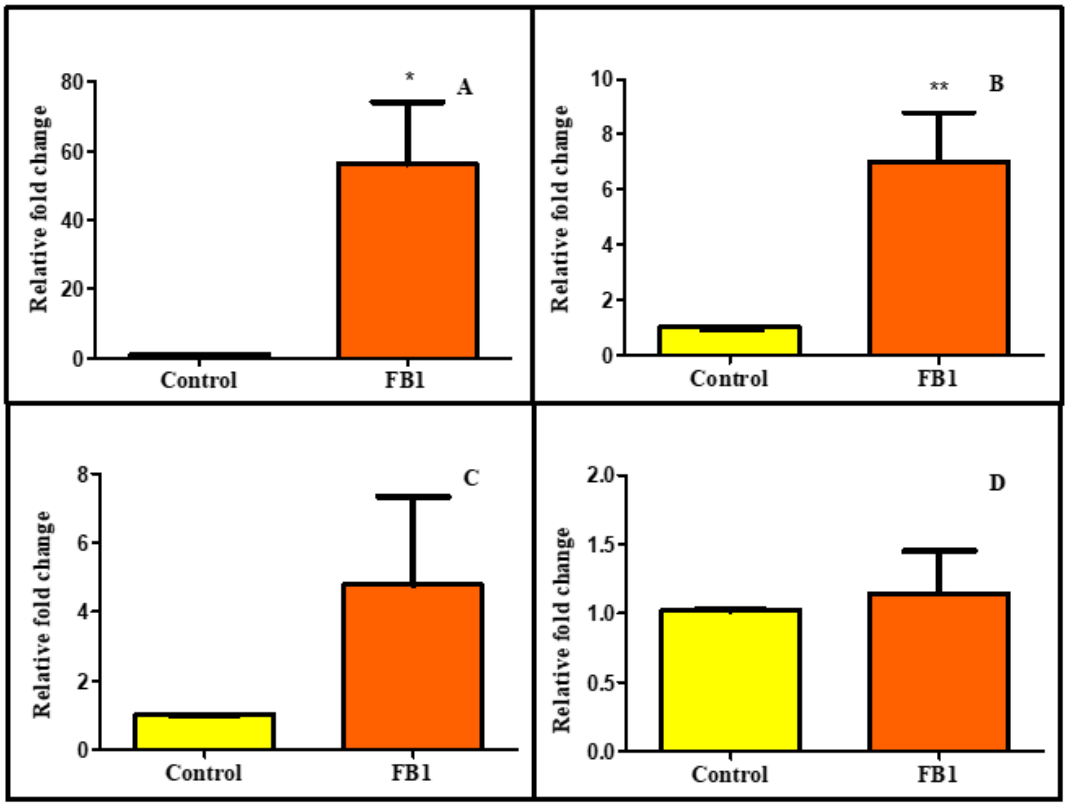

Figure 4.3.2: *DNMTs* and *MBD2* gene expression in lung tissue of the FB1-treated mice relative to the control. A significant upregulation in (A) *DNMT3A* and (B) *DNMT3B* and a non-significant upregulation in (C) *DNMT1* and (D) *MBD2* was present in the lung tissue of treated mice (*p<0.05;**p<0.005).

Chapter 5: Discussion

FB1, produced by the fungus *Fusarium verticillioides*, is a common contaminant of agricultural foods and has been shown to cause numerous health issues (Hopmans and Murphy, 1993, Arumugam *et al*., 2018). This study examined the effects of FB1 on mitochondrial toxicity, along with its influence on oxidative stress, mitophagy, and DNA methylation pathways in the lung tissue of C57BL/6 mice over a 24 hours period, to provide a better understanding of FB1's mechanism of toxicity. The findings revealed a complex interplay between these pathways in the lung tissue of the FB1-treated mice.

FB1 promoted a significant increase in the lipid peroxidation product MDA (Figure 4.1.1) for the lung tissue of the treated mice, this may be a consequence of elevated free radicals such as ROS, as various studies have shown that FB1 can lead to toxicity by promoting increased ROS levels, that damage macromolecules such as lipids (Arumugam *et al*., 2018, Wang *et al*., 2015, Bernabucci *et al*., 2011).

Prior research has demonstrated that FB1 inhibits complex 1 of the ETC, resulting in a loss of mitochondrial membrane potential and elevation in the generation of ROS (Domijan, 2012). The primary defence mechanism against abnormal generation of ROS is provided by antioxidants such as SOD, CAT, and Gpx (Pei *et al*., 2023, Li *et al*., 2015). SOD is the first line of defence and plays a crucial role in the conversion of $O_2^{\bullet-}$ into water and oxygen. In the lung tissue of FB1 treated mice, a notable downregulation of *SOD1* (Figure 4.1.2 B) and a non-significant change in SOD2 gene (Figure 4.1.2 E) and protein (Figure 4.1.3 A) expression was observed. FB1 impairs the ability of SOD1 to effectively detoxify $O_2^{\bullet-}$ in the cytoplasm, resulting in increased $O_2^{\bullet-}$ levels; however, it does not impact the ability of SOD2 to detoxify $O_2^{\bullet-}$ in the mitochondria (Ngo and Duennwald, 2022). Past findings on FB1 and SOD2 also displayed varying results, with a study on HepG2 cells noting an increase in SOD2 gene and protein expression, while studies on brain tissue of FB1-treated mice, Balb/c mice and peripheral blood mononuclear cells found a significant decrease (Arumugam *et al*., 2018, Canan *et al*., 2022, Bernabucci *et al*., 2011, Sibiya, 2018). CAT and Gpx constitute the second tier of defence and collaborate with SOD to diminish abnormal levels of ROS by detoxifying H_2O_2 into water and oxygen (Pei *et al*., 2023, Lü *et al*., 2009). A marked reduction in *Gpx* mRNA expression (Figure 4.1.2 D) as well as CAT gene (Figure 4.1.2 C) and protein (Figure 4.1.3 B) expression in lung tissue of FB1-treated mice suggests that FB1 is downregulating expression of these antioxidants and compromising their ability to counteract the excessive H_2O_2 it is generating. This is in agreement with a study on the effects of FB1 on Balb/c mice and peripheral blood mononuclear cells (Canan *et al*., 2022). In instances where H_2O_2 is not detoxified, it undergoes conversion into hydroxyl radicals (OH•-), resulting in increased oxidative injury (Sibiya, 2018). A marked decline in *Nrf2* gene

expression (Figure 4.1.2 A) was present in the lung tissue of the FB1-treated mice relative to the control group. The reduction in SOD1, CAT and Gpx may be associated with the decrease in *Nrf2* expression, as previous studies have indicated that Nrf2 functions as a transcription factor that interacts with the ARE in the promoter region of genes responsible for encoding these antioxidants (Chen *et al*., 2015). A research investigation that focused on the effects of FB1 on pig iliac endothelial cells revealed that those exposed to FB1 for a duration of 48 hours also exhibited a reduction in Nrf2 as well as in antioxidants, specifically SOD1, SOD2, Gpx, and CAT (Yuan *et al*., 2019). While a study on HepG2 cells noted an increase in Nrf2 levels and a subsequent increase in the antioxidants SOD2, CAT and Gpx gene expression (Arumugam *et al*., 2018). These results suggest that FB1's effects on Nrf2 expression subsequently influence the gene expression of antioxidants. Furthermore, FB1's impact on ROS production and antioxidant defences in the lung tissue of the treated mice are evidence of oxidative stress and are in accordance with numerous previous studies that obtained similar results (Arumugam *et al*., 2018, Sibiya, 2018, Yin *et al*., 1996, Rumora *et al*., 2007).

Oxidative stress has been recognized as a contributor of mitochondrial damage, manifesting through the induction of mitochondrial DNA mutations, disruption of the mitochondrial respiratory chain, changes in membrane permeability and Ca^{++} homeostasis (Guo *et al*., 2013). During stressful conditions, mitochondrial proteins like Sirt3 and Lonp1 are activated to maintain effective functionality. Sirt3 is a deacetylase responsible for modulating the activity of several proteins through both activation and inhibition (Zhang *et al*., 2020). This function allows Sirt3 to play a vital role in mitigating elevated ROS production by regulating mitochondrial homeostasis and enhancing the antioxidant response (Bause and Haigis, 2013). A significant increase in Sirt3 mRNA (Figure 4.2.1 A) and protein (Figure 4.2.2 A) levels was observed for the lung tissue of the FB1-treated mice relative to the control. Similar findings were observed for Sirt3 in HepG2 cells (Arumugam *et al*., 2018). The rise in Sirt3 expression could be interpreted as a protective mechanism activated in response to the oxidative stress generated by FB1. Sirt3 has also been identified as a transcriptional regulator of Lonp1 (Gibellini *et al*., 2014). The downregulation of Lonp1 gene (Figure 4.2.1 B) and protein (Figure 4.2.2 B) expression is indicative of Sirt3 regulating Lonp1 protein expression via deacetylation. Furthermore, Lonp1 is known to assist in the degradation of proteins that have been damaged by oxidative stress or misfolded. The observed inhibition of Lonp1 suggests that exposure to FB1 may result in the build-up of oxidatively damaged proteins within the matrix, contributing to mitochondrial toxicity (Ngo and Duennwald, 2022).

The failure to mitigate mitochondrial toxicity triggers the process of mitophagy which is responsible for the degradation of dysfunctional mitochondria to ensure the preservation of cellular functions (Wen *et al*., 2022). When mitochondrial cells sustain damage or experience a decrease in membrane

potential, Pink1 accumulates around the mitochondria, where it facilitates the initiation of mitophagy (Youle and Narendra, 2010). A notable reduction in the expression of the *Pink1* gene (Figure 4.2.1 C) was observed in the lung tissue of mice treated with FB1. This decline could be attributed to the lowered expression of Nrf2 experienced as existing studies have demonstrated that Nrf2 transcriptionally activates Pink1 (Gumeni *et al*., 2021). The decline in Pink1 expression may have further influenced the significant reduction in Parkin gene (Figure 4.2.1 D) and protein expression (Figure 4.2.2 C) in the lung tissue of FB1-treated mice. This is attributed to the requirement of Pink1's accumulation on the outer mitochondrial membrane to activate Parkin, which subsequently triggers mitophagy by ubiquitinating multiple proteins present on the outer mitochondrial membrane (Geisler *et al*., 2010). One of the proteins Parkin ubiquitinates is p62, which is in the cytoplasm and serves as a crucial regulator functioning as a selective autophagy receptor. This receptor facilitates the degradation of substrates that have undergone ubiquitination (Gureev *et al*., 2020). A significant downregulation of *p62* mRNA (Figure 4.2.1 E) expression was noted in the lung tissue of the FB1-treated mice. This occurrence may be linked to diminished Nrf2 levels in the treated lung tissue as past studies have indicated that the transcription of p62 is activated during oxidative stress through the binding of Nrf2 to the ARE located in the p62 promoter (Jain *et al*., 2015). Thus, it can be reasoned that the impairment of Nrf2 by FB1 resulted in the reduction of *p62* gene expression. The diminished expression of Pink1, Parkin and p62 in the tissues of the treated mice suggest that FB1 interferes with the process of mitophagy thereby, hindering the removal of damaged mitochondria through the downregulation of vital mitogenic promoters, and further contributes to mitochondrial toxicity in the mice lung tissue. An examination of the effects of FB1 on mitophagy in the kidney tissues of mice revealed that FB1 led to an increased expression of genes and proteins related to mitophagy (Ping *et al*., 2024).

DNA methylation is a vital epigenetic mechanism involving the enzymatic transfer of methyl groups derived from SAM to the C-5 region of the cytosine ring present in DNA, by enzymes known as DNMTs (García-Guede *et al*., 2020, Jin *et al*., 2011, Menezo *et al*., 2016). This investigation revealed a significant increase in global DNA methylation levels (Figure 4.3.1). This idea is further reinforced by the significant increase in *DNMT3A* (Figure 4.3.2 A) and *DNMT3B* (Figure 4.3.2 B) gene expression and the non-significant increase in *DNMT1* gene expression (Figure 4.3.2 C) in the lung tissue of FB1-treated mice. A non-significant change in the demethylation enzyme *MBD2* (Figure 4.3.2 D), which functions by binding to the CpG islands in the promoter regions was also observed (Berger and Bird, 2005). An earlier study examining the potential of FB1 to trigger global DNA methylation in HepG2 cells produced results that diverged from those of the current study, with a decrease in DNMT1, DNMT3A and DNMT3B expression as well as an increase in MBD2 expression

(Chuturgoon *et al*., 2014). The study went on to conclude that FB1 induced global hypomethylation in HepG2 cells. An earlier examination of rat C6 glioma cells produced findings similar to those of this study, showing that a 24-hours exposure to FB1 induced DNA hypermethylation (Arumugam *et al*., 2021). Furthermore, the study observed that hypermethylation was not induced in C6 glioma cells subjected to elevated concentrations, proposing that the lack of DNA hypermethylation at higher concentrations may be a result of increased toxicity and DNA damage caused by FB1.

The occurrence of DNA hypermethylation in the lung tissue may be attributed to the FB1-induced oxidative stress. A key characteristic of oxidative stress is increased ROS generation, which prior research has demonstrated to influence DNA methylation levels (Gao *et al*., 2019). H_2O_2 serves as an example of ROS that influences DNA methylation by deprotonating cytosine at the C-5 position by functioning as a nucleophile, thereby accelerating the interaction between DNA and SAM (Gao *et al*., 2019). Additionally, ROS can regulate the expression of DNMTs. The superoxide anion, in particular, has been shown to promote the expression of DNMTs, with previous studies establishing a direct relationship between heightened superoxide levels and the increased expression of DNMT1 and DNMT3B (Campos *et al*., 2007). Thus, one may deduce that FB1's role in enhancing the production of ROS, such as O^{-2} and H_2O_2, as well as its suppression of antioxidant expression, particularly SOD1 and CAT, in the lung tissue of the mice treated with FB1, could have contributed to the phenomenon of DNA hypermethylation, through the acceleration of the DNA methylation reaction and increased expression of DNMTs. The occurrence of DNA hypermethylation has been associated with genomic instability, a factor closely linked to the initiation of cancer (Mobio *et al*., 2000, Kouadio *et al*., 2007). Previous studies on FB1 have also identified this mycotoxin as an epigenetic carcinogen (Fragou *et al*., 2011). Consequently, it is plausible that DNA hypermethylation resulting from oxidative stress induced by FB1 may contribute to the emergence of lung cancer.

In summary, the exposure to FB1 led to oxidative stress (Figure 5.1) characterized by elevated ROS production and a reduction in antioxidant defences. This disruption affected mitochondrial homeostasis, compromising mechanisms such as mitochondrial stress response proteins and mitophagy, ultimately resulting in mitochondrial dysfunction. Additionally, the oxidative stress induced by FB1 contributed to global DNA hypermethylation in the lung tissue by enhancing the rate of the DNA methylation process and upregulating DNMT expression.

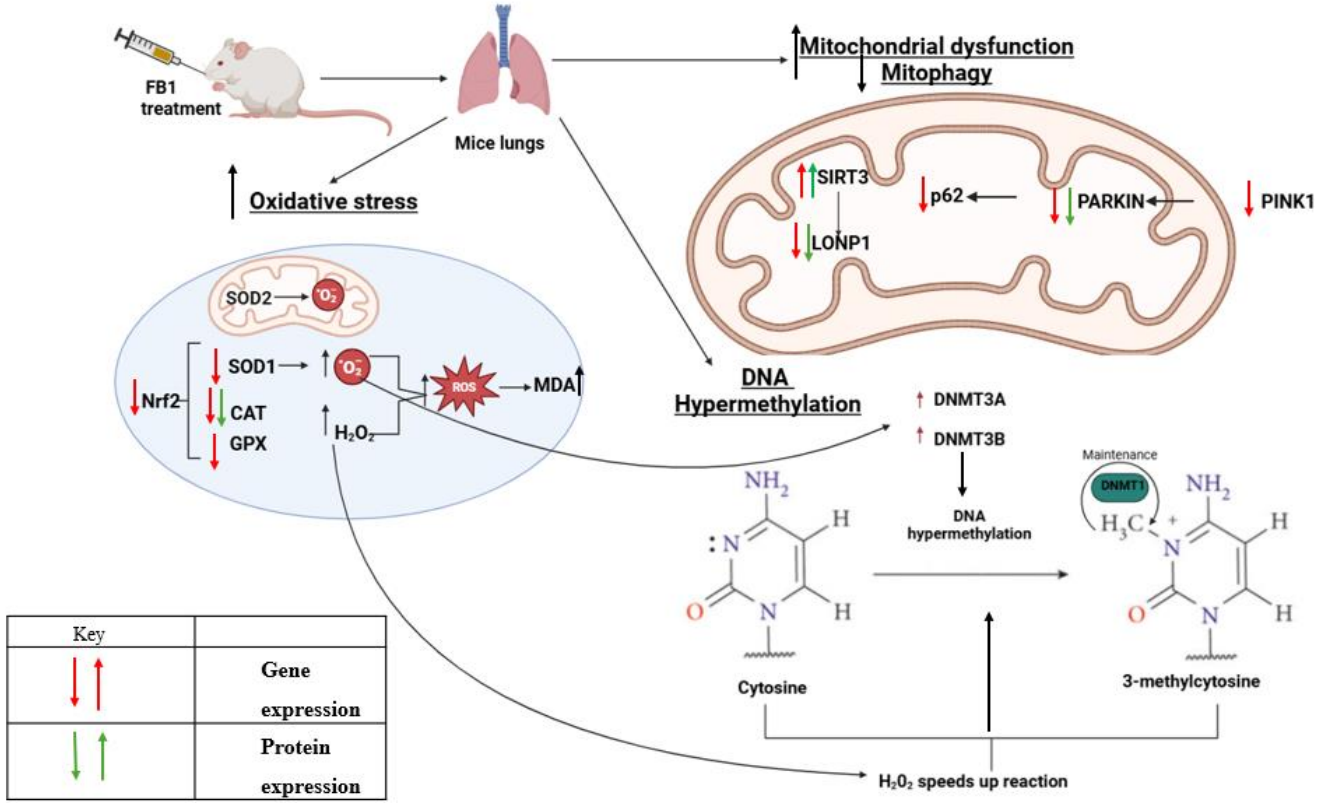

Figure 5.1: A summary of the results presented in this study (prepared by author).

Chapter 6: Conclusion

A large population of humans and animals that consume agricultural goods contaminated by the *Fusarium* mycotoxin FB1 have reported experiencing critical health issues. To effectively develop treatments for these health concerns, it is essential to gain a deeper understanding of the molecular and cellular mechanisms associated with FB1. Past studies have identified FB1 as a possible inducer of mitochondrial toxicity. This study aimed to examine the influence of FB1 on the mitochondria in the lung tissue of FB1-treated mice, while also exploring the pathways of oxidative stress, mitophagy and DNA methylation and how they contribute to toxicity.

FB1 induced oxidative stress in the mice lung tissue through an increase in ROS production and a reduction in antioxidant defences, which subsequently resulted in an increase in mitochondrial Sirt3 levels and disrupted the expression of proteins that mitigate mitochondrial stress, such as Lonp1. Consequently, the mitochondria within the tissue were unable to maintain homeostasis, as FB1 obstructed the mitophagy process, leading to further mitochondrial dysfunction. Ultimately, the oxidative stress induced by FB1 was shown to result in global DNA hypermethylation, which may contribute to the potential development of FB1-related toxicity or lung cancer.

These results provide significant insights into the molecular and cellular mechanisms associated with FB1. Its capacity to induce toxicity through oxidative stress, mitochondrial dysfunction, and mitophagy is clearly demonstrated. However, further investigation is necessary to elucidate how hypermethylation resulting from FB1-induced oxidative stress may contribute to carcinogenic effects in lung tissue.

Limitations and Recommendations

This was a pilot investigation on mice that were exposed to FB1 for 24 hours. For future studies, it would be beneficial to work with more mice that have been exposed to FB1 for extended incubation times. This could provide a clearer picture of FB1's toxicity. Another limitation was that mitochondrial function could not be assessed directly by measuring ATP production and membrane potential due to the experiment using frozen tissue samples. Moving forward, it will be beneficial to isolate mitochondria from the lung tissue and evaluate mitochondrial function. Further studies should also look at the effects of FB1 on other epigenetic modifications in lung tissues. As well as incorporate extended exposure durations and the use of alternative cell lines to elucidate these pathways of toxicity. Future research utilising an in vivo model is also warranted, to substantiate the mechanism of FB1-induced toxicity.

References

ABCAM 2024. Global DNA Methylation Assay Kit (5 Methyl Cytosine, Colorimetric) (ab233486) | Abcam. *Abcam.com*.

AHMAD, M., WOLBERG, A. & KAHWAJI, C. I. 2018. Biochemistry, electron transport chain.

ALHAJJ, M., FARHANA, A. & ZUBAIR, M. 2023. Enzyme Linked Immunosorbent Assay (ELISA). *PubMed*.

ALIZADEH, A. M., ROHANDEL, G., ROUDBARMOHAMMADI, S., ROUDBARY, M., SOHANAKI, H., GHIASIAN, S. A., TAHERKHANI, A., SEMNANI, S. & AGHASI, M. 2012. Fumonisin B1 Contamination of Cereals and Risk of Esophageal Cancer in a High Risk Area in Northeastern Iran. *Asian Pacific Journal of Cancer Prevention,* 13**,** 2625-2628.

ALVITO, P., ASSUNÇÃO, R. M., BAJARD, L., MARTINS, C., MENGELERS, M. J., MOL, H., NAMORADO, S., VAN DEN BRAND, A. D., VASCO, E. & VIEGAS, S. 2022. Current Advances, Research Needs and Gaps in Mycotoxins Biomonitoring under the HBM4EU—Lessons Learned and Future Trends. *Toxins,* 14**,** 826.

ARUMUGAM, T., GHAZI, T. & CHUTURGOON, A. A. 2021. Molecular and epigenetic modes of Fumonisin B₁ mediated toxicity and carcinogenesis and detoxification strategies. *Critical reviews in toxicology,* 51**,** 76-94.

ARUMUGAM, T., PILLAY, Y., GHAZI, T., NAGIAH, S., ABDUL, N. S. & CHUTURGOON, A. A. 2018. Fumonisin B1-induced oxidative stress triggers Nrf2-mediated antioxidant response in human hepatocellular carcinoma (HepG2) cells. *Mycotoxin Research,* 35**,** 99-109.

BACCARELLI, A. & BOLLATI, V. 2009. Epigenetics and environmental chemicals. *Current Opinion in Pediatrics,* 21**,** 243-251.

BAIRD, L. & YAMAMOTO, M. 2020. The Molecular Mechanisms Regulating the KEAP1-NRF2 Pathway. *Molecular and Cellular Biology,* 40.

BAUSE, A. S. & HAIGIS, M. C. 2013. SIRT3 regulation of mitochondrial oxidative stress. *Experimental Gerontology,* 48**,** 634-639.

BERGER, J. & BIRD, A. 2005. Role of MBD2 in gene regulation and tumorigenesis. *Biochemical Society Transactions,* 33**,** 1537-1540.

BERNABUCCI, U., COLAVECCHIA, L., DANIELI, P. P., BASIRICÒ, L., LACETERA, N., NARDONE, A. & RONCHI, B. 2011. Aflatoxin B1 and fumonisin B1 affect the oxidative status of bovine peripheral blood mononuclear cells. *Toxicology in Vitro,* 25**,** 684-691.

BURTON, G. J. & JAUNIAUX, E. 2011. Oxidative stress. *Best Practice & Research Clinical Obstetrics & Gynaecology,* 25**,** 287-299.

BUSH, B. J., CARSON, M. L., CUBETA, M. A., HAGLER, W. M. & PAYNE, G. A. 2004. Infection and Fumonisin Production by Fusarium verticillioides in Developing Maize Kernels. *Phytopathology,* 94**,** 88-93.

BYJU'S 2023. Lungs Diagram - Human Lungs Anatomy. *BYJUS*.

CAMPOS, A. C. E., MOLOGNONI, F., MELO, F. H. M., GALDIERI, L. C., CARNEIRO, C. R. W., D'ALMEIDA, V., CORREA, M. & JASIULIONIS, M. G. 2007. Oxidative Stress Modulates DNA Methylation during Melanocyte Anchorage Blockade Associated with Malignant Transformation. *Neoplasia,* 9**,** 1111-1121.

CANAN, G., YALCIN, R., KART, A., EMINE, A., TUMAKOVICH, M. Z. & ONUR, A. 2022. The effects of resveratrol on SIRT2, SIRT3 expression levels and oxidative DNA damage in fumonisin-induced hepatotoxicity in BALB/c mice. *Veterinarski arhiv,* 92**,** 97-108.

CAYMAN, C. 2022. picking an oxidative damage assay. *www.caymanchem.com*.

CHEN, B., LU, Y., CHEN, Y. & CHENG, J. 2015. The role of Nrf2 in oxidative stress-induced endothelial injuries. *Journal of Endocrinology,* 225**,** R83-R99.

CHEN, J., WEI, Z., WANG, Y., LONG, M., WU, W. & KUCA, K. 2021. Fumonisin B1: Mechanisms of toxicity and biological detoxification progress in animals. *Food and Chemical Toxicology,* 149**,** 111977.

CHUTURGOON, A., PHULUKDAREE, A. & DEVAPREGASAN, M. 2014. Fumonisin B1 induces global DNA hypomethylation in HepG2 cells – An alternative mechanism of action. *Toxicology,* 315**,** 65-69.

CLINISCIENCES 2024. Experimental Protocol for Western Blotting Clinisciences. *Clinisciences.com.*

DE LEON, J. A. D. & BORGES, C. R. 2020. Evaluation of Oxidative Stress in Biological Samples Using the Thiobarbituric Acid Reactive Substances Assay. *Journal of Visualized Experiments*.

DOMIJAN, A.-M. 2012. Fumonisin B1: A Neurotoxic Mycotoxin / Fumonizin B1: Neurotoksični Mikotoksin. *Archives of Industrial Hygiene and Toxicology,* 63**,** 531-544.

DOMIJAN, A.-M., STJEPANA, K. & ABRAMOV, Y. A. 2012. Impact of fumonisin B1 on glutamate toxicity and low magnesium-induced seizure activity in neuronal primary culture. *Neuroscience,* 202**,** 10-16.

FANG, T., WANG, M., XIAO, H. & WEI, X. 2019. Mitochondrial dysfunction and chronic lung disease. *Cell Biology and Toxicology,* 35**,** 493-502.

FRAGOU, D., FRAGOU, A., KOUIDOU, S., NJAU, S. & KOVATSI, L. 2011. Epigenetic mechanisms in metal toxicity. *Toxicology Mechanisms and Methods,* 21**,** 343-352.

GAO, X., ZHANG, Y., BURWINKEL, B., XUAN, Y., HOLLECZEK, B., BRENNER, H. & SCHOTTKER, B. 2019. The associations of DNA methylation alterations in oxidative stress-related genes with cancer incidence and mortality outcomes: a population-based cohort study. *Clin Epigenetics,* 11**,** 14.

GAO, Z., LUO, K., ZHU, Q., PENG, J., LIU, C., WANG, X., LI, S. & ZHANG, H. 2023. The natural occurrence, toxicity mechanisms and management strategies of Fumonisin B1 : A review. *Environmental Pollution (Barking, Essex: 1987),* 320**,** 121065.

GARCÍA-GUEDE, Á., VERA, O. & IBÁÑEZ-DE-CACERES, I. 2020. When Oxidative Stress Meets Epigenetics: Implications in Cancer Development. *Antioxidants,* 9**,** 468.

GAVINI, K. & PARAMESHWARAN, K. 2025. Western Blot. *StatPearls.* Treasure Island (FL).

GEISLER, S., HOLMSTRÖM, K. M., TREIS, A., SKUJAT, D., WEBER, S. S., FIESEL, F. C., KAHLE, P. J. & SPRINGER, W. 2010. The PINK1/Parkin-mediated mitophagy is compromised by PD-associated mutations. *Autophagy,* 6**,** 871-878.

GELDERBLOM, W. C. A., MARASAS, W. F. O., LEBEPE-MAZUR, S., SWANEVELDER, S. & ABEL, S. 2008. Cancer initiating properties of fumonisin B1 in a short-term rat liver carcinogenesis assay. *Toxicology,* 250**,** 89-95.

GHAZI, T. 2019. Fusaric acid-induced promoter methylation of DNA methyltransferases triggers DNA hypomethylation in human hepatocellular carcinoma (HepG2) cells. *Google.co.za*.

GIBELLINI, L., PINTI, M., BERETTI, F., CIRO LEONARDO, P., ONOFRIO, A., RICCIO, M., CARNEVALE, G., SARA DE, B., NASI, M., TORELLI, F., FEDERICA, B., ANTO DE, P. & COSSARIZZA, A. 2014. Sirtuin 3 interacts with Lon protease and regulates its acetylation status. 18**,** 76-81.

GOKSUN, D., BUKET, A. & SIBEL, O. 2015. Role of fumonisin B1 on DNA methylation changes in rat kidney and liver cells. *Pharmaceutical biology,* 53**,** 1302-1310.

GUMENI, S., PAPANAGNOU, E.-D., MANOLA, M. S. & TROUGAKOS, I. P. 2021. Nrf2 activation induces mitophagy and reverses Parkin/Pink1 knock down-mediated neuronal and muscle degeneration phenotypes. *Cell Death & Disease,* 12.

GUO, C., SUN, L., CHEN, X. & ZHANG, D. 2013. Oxidative stress, mitochondrial damage and neurodegenerative diseases. *Neural regeneration research,* 8.

GUPTA, S. V., CAMPOS, L. & KRISTINA HILDEGARD, S. 2023. Mitochondrial superoxide dismutase Sod2 suppresses nuclear genome instability during oxidative stress. *Genetics,* 225.

GUREEV, A. P., SADOVNIKOVA, I. S., STARKOV, N. N., STARKOV, A. A. & POPOV, V. N. 2020. p62-Nrf2-p62 Mitophagy Regulatory Loop as a Target for Preventive Therapy of Neurodegenerative Diseases. *Brain Sciences,* 10**,** 847.

HASCHEK, W. M., GUMPRECHT, L. A., SMITH, G., TUMBLESON, M. E. & CONSTABLE, P. D. 2001. Fumonisin toxicosis in swine: an overview of porcine pulmonary edema and current perspectives. *Environmental Health Perspectives,* 109**,** 251-257.

HOPMANS, E. C. & MURPHY, P. A. 1993. Detection of fumonisins B1, B2, and B3 and hydrolyzed fumonisin B1 in corn-containing foods. *Journal of Agricultural and Food Chemistry,* 41**,** 1655-1658.

HUSSEIN, H. 2001. Toxicity, metabolism, and impact of mycotoxins on humans and animals. *Toxicology,* 167**,** 101-134.

IARC 2002. *Some Traditional Herbal Medicines, Some Mycotoxins, Naphthalene and Styrene*.

JAIN, A., RUSTEN, T. E., KATHEDER, N., ELVENES, J., BRUUN, J.-A., SJØTTEM, E., LAMARK, T. & JOHANSEN, T. 2015. p62/Sequestosome-1, Autophagy-related Gene 8, and Autophagy inDrosophilaAre Regulated by Nuclear Factor Erythroid 2-related Factor 2 (NRF2), Independent of Transcription Factor TFEB. *Journal of Biological Chemistry,* 290**,** 14945-14962.

JIN, B., LI, Y. & ROBERTSON, K. D. 2011. DNA Methylation: Superior or Subordinate in the Epigenetic Hierarchy? *Genes & Cancer,* 2**,** 607-617.

KAMLE, M., MAHATO, D. K., DEVI, S., LEE, K. E., KANG, S. G. & KUMAR, P. 2019. Fumonisins: Impact on Agriculture, Food, and Human Health and their Management Strategies. *Toxins,* 11**,** 328.

KHAN, R. B., PHULUKDAREE, A. & CHUTURGOON, A. A. 2018. Fumonisin B1 induces oxidative stress in oesophageal (SNO) cancer cells. *Toxicon,* 141**,** 104-111.

KOUADIO, J. H., DANO, S. D., MOUKHA, S., MOBIO, T. A. & CREPPY, E. E. 2007. Effects of combinations of Fusarium mycotoxins on the inhibition of macromolecular synthesis, malondialdehyde levels, DNA methylation and fragmentation, and viability in Caco-2 cells. *Toxicon,* 49**,** 306-317.

LI, S., TAN, H.-Y., WANG, N., ZHANG, Z.-J., LAO, L., WONG, C.-W. & FENG, Y. 2015. The Role of Oxidative Stress and Antioxidants in Liver Diseases. *International Journal of Molecular Sciences,* 16**,** 26087-26124.

LIU, H.-Y. 2023. Lipid Peroxidation in Oxidative Stress, Inflammation, and Cell Death. *Hindawi*.

LIVAK, K. J. & SCHMITTGEN, T. D. 2001. Analysis of Relative Gene Expression Data Using Real-Time Quantitative PCR and the 2−ΔΔCT Method. *Methods,* 25**,** 402-408.

LÜ, J.-M., LIN, P. H., YAO, Q. & CHEN, C. 2009. Chemical and molecular mechanisms of antioxidants: experimental approaches and model systems. *Journal of Cellular and Molecular Medicine,* 14**,** 840-860.

MALHOTRA, B. D., SRIVASTAVA, S., ALI, M. A. & SINGH, C. 2014. Nanomaterial-Based Biosensors for Food Toxin Detection. *Applied Biochemistry and Biotechnology,* 174**,** 880-896.

MENEZO, Y. J. R., SILVESTRIS, E., DALE, B. & ELDER, K. 2016. Oxidative stress and alterations in DNA methylation: two sides of the same coin in reproduction. *Reproductive BioMedicine Online,* 33**,** 668-683.

MERRILL, A. H., SULLARDS, M. C., WANG, E., VOSS, K. A. & RILEY, R. T. 2001. Sphingolipid metabolism: roles in signal transduction and disruption by fumonisins. *Environmental Health Perspectives,* 109**,** 283-289.

MOBIO, T. A., ANANE, R., BAUDRIMONT, I., MARIA ROSARIA, C., SHIER, T. W., DANO, S. D., UENO, Y. & CREPPY, E. E. 2000. Epigenetic Properties of Fumonisin B1: Cell Cycle Arrest and DNA Base Modification in C6 Glioma Cells. *Toxicology and Applied Pharmacology,* 164**,** 91-96.

MOHAN, J., SHEIK ABDUL, N., NAGIAH, S., GHAZI, T. & CHUTURGOON, A. A. 2022. Fumonisin B2 Induces Mitochondrial Stress and Mitophagy in Human Embryonic Kidney (Hek293) Cells—A Preliminary Study. *Toxins,* 14**,** 171.

NARENDRA, D., KANE, L. A., HAUSER, D. N., FEARNLEY, I. M. & YOULE, R. J. 2010. p62/SQSTM1 is required for Parkin-induced mitochondrial clustering but not mitophagy; VDAC1 is dispensable for both. *Autophagy,* 6**,** 1090-1106.

NATIONAL HEART, L. & BLOOD, I. 2022. How the Lungs Work - The Lungs | NHLBI, NIH. *www.nhlbi.nih.gov*.

NGO, V. & DUENNWALD, M. L. 2022. Nrf2 and Oxidative Stress: A General Overview of Mechanisms and Implications in Human Disease. *Antioxidants,* 11**,** 2345.

NOWAKOWSKI, A. B., WOBIG, W. J. & PETERING, D. H. 2014. Native SDS-PAGE: high resolution electrophoretic separation of proteins with retention of native properties including bound metal ions. *Metallomics,* 6**,** 1068-1078.

OMOTAYO, O. P., OMOTAYO, A. O., MWANZA, M. & BABALOLA, O. O. 2019. Prevalence of Mycotoxins and Their Consequences on Human Health. *Toxicological Research,* 35**,** 1-7.

PEI, J., PAN, X., WEI, G. & HUA, Y. 2023. Research progress of glutathione peroxidase family (GPX) in redoxidation. *Frontiers in Pharmacology,* 14.

PHANIENDRA, A., JESTADI, D. B. & PERIYASAMY, L. 2014. Free Radicals: Properties, Sources, Targets, and Their Implication in Various Diseases. *Indian Journal of Clinical Biochemistry,* 30**,** 11-26.

PIECZENIK, S. R. & NEUSTADT, J. 2007. Mitochondrial dysfunction and molecular pathways of disease. *Experimental and Molecular Pathology,* 83**,** 84-92.

PING, Z., ZHANG, S., DU, X., KEHE, H., CHEN, X. & WANG, C. 2024. Mitophagy-regulated Necroptosis plays a vital role in the nephrotoxicity of Fumonisin B1 in vivo and in vitro. *Food and Chemical Toxicology,* 189**,** 114714-114714.

PROTEOMICS, C. 2024. Protocol for Bicinchoninic Acid (BCA) Protein Assay. *Creative Proteomics*.

QAZI, M. A. 2018. Welcome to American Journal of Pharmacy and Health Research. *www.ajphr.com*.

RHEEDER, J. P., MARASAS, W. F. O. & VISMER, H. F. 2002. Production of Fumonisin Analogs by Fusarium Species. *Applied and Environmental Microbiology,* 68**,** 2101-2105.

RILEY, R. T. & MERRILL, A. H. 2019. Ceramide synthase inhibition by fumonisins: a perfect storm of perturbed sphingolipid metabolism, signaling, and disease. *Journal of Lipid Research,* 60**,** 1183-1189.

RUMORA, L., DOMIJAN, A.-M., GRUBIŠIĆ, T. Ž. & PERAICA, M. 2007. Mycotoxin fumonisin B1 alters cellular redox balance and signalling pathways in rat liver and kidney. *Toxicology,* 242**,** 31-38.

SHEIK ABDUL, N. & MARNEWICK, J. L. 2020. Fumonisin B1-induced mitochondrial toxicity and hepatoprotective potential of rooibos: An update. *Journal of Applied Toxicology,* 40**,** 1602-1613.

SHEPHARD, G. S., THIEL, P. G., STOCKENSTRÖM, S. & SYDENHAM, E. W. 1996. Worldwide survey of fumonisin contamination of corn and corn-based products. *Journal of AOAC International,* 79**,** 671-687.

SHIN, M., WATSON, E. R., SONG, A. S., MINDREBO, J. T., NOVICK, S. J., GRIFFIN, P. R., WISEMAN, R. L. & LANDER, G. C. 2021. Structures of the human LONP1 protease reveal regulatory steps involved in protease activation. *Nature Communications,* 12**,** 3239.

SIBIYA, T. 2018. Fumonisin B1 induced antioxidant response in C57BL/6 male mice brain. *Ukzn.ac.za*.

STEWARD, K. 2022. qPCR Analysis, How a qPCR Machine Works and qPCR Protocol. *Analysis & Separations from Technology Networks*.

STOEV, S. D. 2015. Foodborne mycotoxicoses, risk assessment and underestimated hazard of masked mycotoxins and joint mycotoxin effects or interaction. *Environmental Toxicology and Pharmacology,* 39**,** 794-809.

SURESHBABU, A. & BHANDARI, V. 2013. Targeting mitochondrial dysfunction in lung diseases: emphasis on mitophagy. *Frontiers in Physiology,* 4.

VENDRUSCOLO, C. P., FRIAS, N. C., CARVALHO, C. B., SÁ, L. R. M., BELLI, C. B. & BACCARIN, R. Y. A. 2016. Leukoencephalomalacia Outbreak in Horses due to Consumption of Contaminated Hay. *Journal of Veterinary Internal Medicine,* 30**,** 1879-1881.

VIKAS, A. 2018. Oxidative stress in chronic lung disease: From mitochondrial dysfunction to dysregulated redox signaling. *Molecular Aspects of Medicine,* 63**,** 59-69.

WAES, J. G.-V., VOSS, K. A., STEVENS, V. J., SPEER, M. C. & RILEY, R. T. 2009. Chapter 5 Maternal Fumonisin Exposure as a Risk Factor for Neural Tube Defects. *Elsevier eBooks***,** 145-181.

WALKER, D. 2022. The Lungs - Position - Structure - TeachMeAnatomy. *Teachmeanatomy.info*.

WANG, X., WU, Q., WAN, D., LIU, Q., CHEN, D., LIU, Z., MARTÍNEZ-LARRAÑAGA, M. R., MARTÍNEZ, M. A., ANADÓN, A. & YUAN, Z. 2015. Fumonisins: oxidative stress-mediated toxicity and metabolism in vivo and in vitro. *Archives of Toxicology,* 90**,** 81-101.

WEIR, H. J. M., LANE, J. D. & BALTHASAR, N. 2013. SIRT3. *Genes & Cancer,* 4**,** 118-124.

WEN, J., PAN, T., LI, H., CHEN, F., CAI, Z. & ZHAO, B. 2022. Role of mitophagy in the hallmarks of aging Running title: Mitophagy in aging. *The Journal of Biomedical Research,* 37**,** 1.

WORLD HEALTH, O. 2023. Mycotoxins. *Who.int*.

YAZAR, S. & OMURTAG, G. 2008. Fumonisins, Trichothecenes and Zearalenone in Cereals. *International Journal of Molecular Sciences,* 9**,** 2062-2090.

YILDIRIM, R. M., ERGUN, Y. & BASAR, M. 2022. Mitochondrial Dysfunction, Mitophagy and Their Correlation with Perinatal Complications: Preeclampsia and Low Birth Weight. *Biomedicines,* 10**,** 2539.

YIN, J.-J., SMITH, M. J., EPPLEY, R. M., PAGE, S. W. & SPHON, J. A. 1996. Effects of Fumonisin B1on Oxygen Transport in Membranes. *Biochemical and Biophysical Research Communications,* 225**,** 250-255.

YOULE, R. J. & NARENDRA, D. P. 2010. Mechanisms of mitophagy. *Nature Reviews Molecular Cell Biology,* 12**,** 9-14.

YUAN, Q., JIANG, Y., FAN, Y., MA, Y., LEI, H. & SU, J. 2019. Fumonisin B1 Induces Oxidative Stress and Breaks Barrier Functions in Pig Iliac Endothelium Cells. *Toxins,* 11**,** 387.

ZANINI, G., SELLERI, V., MALERBA, M., KATERYNA, S., GIORGIA, S., NASI, M., ANNA VITTORIA, M. & PINTI, M. 2023. The Role of Lonp1 on Mitochondrial Functions during Cardiovascular and Muscular Diseases. *Antioxidants*, 12**,** 598-598.

ZHAN, B. & SHEN, J. 2022. Mitochondria and their potential role in acute lung injury (Review). *Experimental and Therapeutic Medicine,* 24.

ZHANG, J., XIANG, H., LIU, J., CHEN, Y., HE, R.-R. & LIU, B. 2020. Mitochondrial Sirtuin 3: New emerging biological function and therapeutic target. *Theranostics,* 10**,** 8315-8342.

Appendix A

There was a significant decrease in *NQO1* (p=0.0084) (Figure 5.1) gene expression in lung tissue of FB1-treated mice. NQO1 is induced as a part of the Nrf2-directed adaptive response to cellular stress including oxidative stress. Therefore, decreased *NQO1* gene expression may be a result of decreased *Nrf2* gene expression, which may ultimately contribute to oxidative stress.

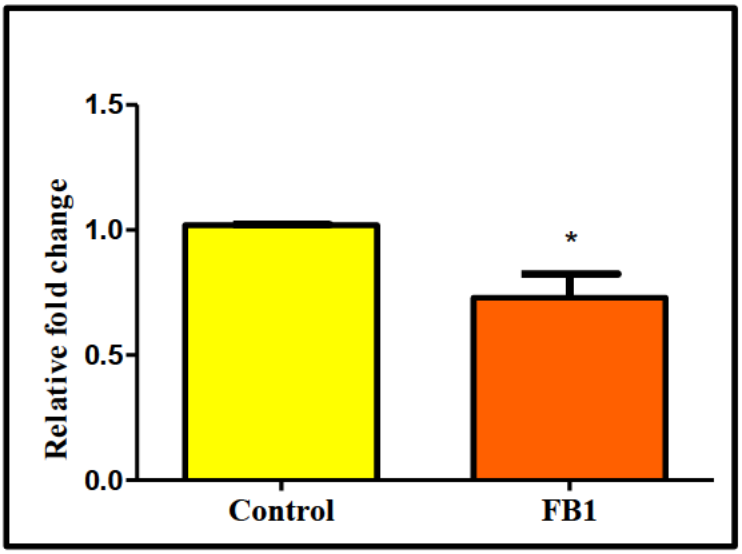

Figure 6.1: NQO1 gene expression in lung tissue of the FB1-treated mice compared to the control. A significant upregulation in *NQO1* gene expression was present for the lung tissue of the FB1-treated mice relative to the control (*p<0.05).

Appendix B

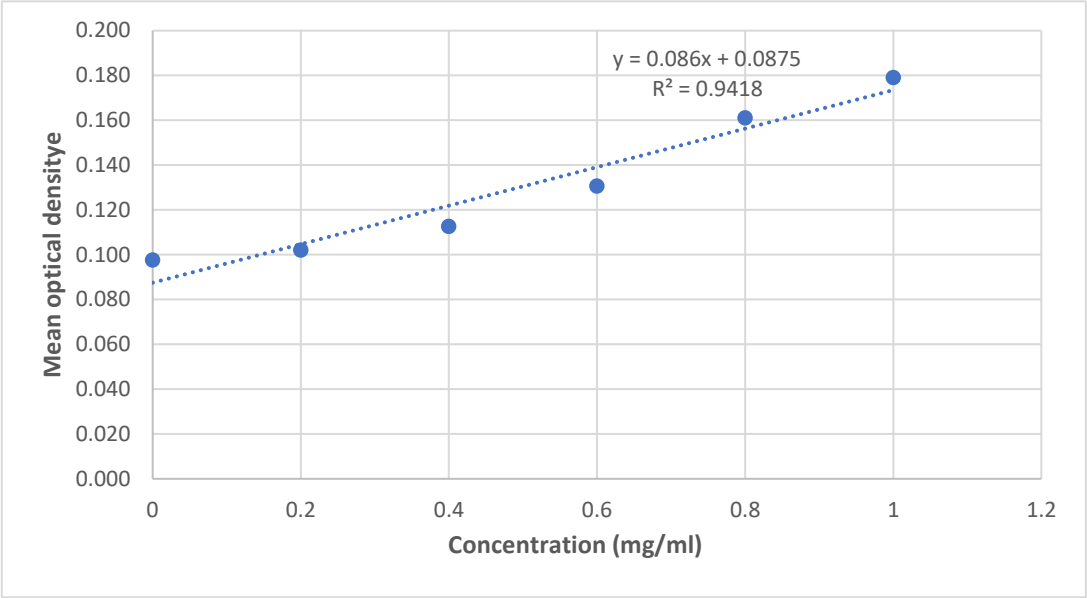

Figure 7.1: A standard curve illustrating the known concentrations of bovine serum albumin (BSA) used to quantify the protein concentration in each sample.

Appendix C

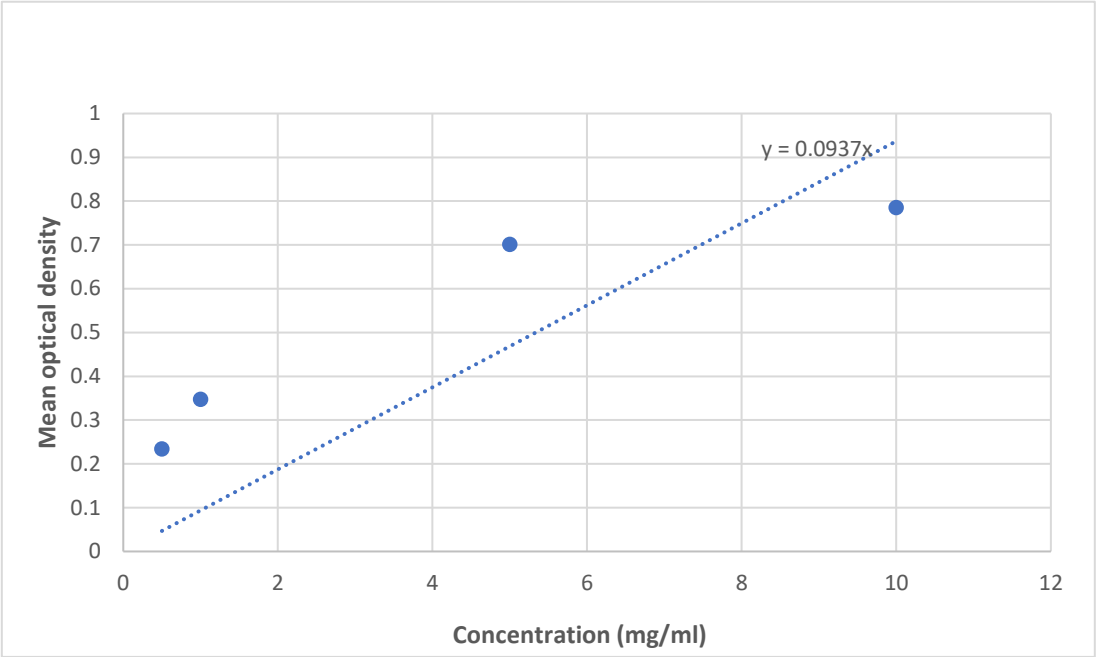

Figure 8.1: Standard curve used to quantify global DNA methylation levels.